A DISSERTATION ON

Identifying Potential Inhibitors of Human Epidermal Growth Factor Receptor 2 using Structure-Based Virtual Screening, Docking, Molecular Dynamics Simulations and Principal Component Analysis

SUBMITTED TO THE
DEPARTMENT OF BIOENGINEERING
FACULTY OF ENGINEERING
INTEGRAL UNIVERSITY, LUCKNOW

IN PARTIAL FULFILMENT
FOR THE
DEGREE OF MASTER OF TECHNOLOGY
IN BIOTECHNOLOGY

BY
Heena Bano
M. Tech Biotechnology (IV Semester)
Roll No: 2001361009

UNDER THE SUPERVISION OF

Dr. Mohammad Kalim Ahmad Khan
Associate Professor
Department of Bioengineering

INTEGRAL UNIVERSITY, DASAULI, KURSI ROAD
LUCKNOW- 226026

DECLARATION FORM

I, **Heena Bano**, a student of **M. Tech Biotechnology** (2nd Year/ 4th Semester), Integral University have completed my six months dissertation work entitled **"Potential Inhibitors of Human Epidermal Growth Factor Receptor 2 using Structure-Based Virtual Screening, Docking, Molecular Dynamics Simulations and Principal Component Analysis"** successfully from IIRC 7, Integral University, Lucknow under the able guidance of **Dr. Mohammad Kalim Ahmad Khan.**

I, hereby, affirm that the work has been done by me in all aspects. I have sincerely prepared this project report and the results reported in this study are genuine and authentic.

Heena Bano

Date:

Dr. Salman Akhtar

Course Coordinator

Date:

INTEGRAL UNIVERSITY

Established Under the Integral University Act 2004 (U.P. Act No.9 of 2004)
Approved by University Grant Commission
Phone No.: +91(0522) 2890812, 2890730, 3296117, 6451039, Fax No.: 0522-2890809
Kursi Road, Lucknow-226026 Uttar Pradesh (INDIA)

CERTIFICATE BY SUPERVISOR

It is hereby certified that **Ms. Heena Bano** (Enrollment Number 2000101174) has carried out the research work presented in this thesis entitled **"Potential Inhibitors of Human Epidermal Growth Factor Receptor 2 using Structure-Based Virtual Screening, Docking, Molecular Dynamics Simulations and Principal Component Analysis"** for the award of **M. Tech Biotechnology** from Integral University, Lucknow under my supervision. The thesis embodies results of original work and studies carried out by the student herself and the contents of the thesis do not form the basis for the award of any other degree to the candidate or to anybody else from this or any other University. The dissertation was a compulsory part of her **M. Tech Biotechnology**.

I wish her good luck and bright future.

Dr. Mohammad Kalim Ahmad Khan.
Associate Professor
Department of Bioengineering

INTEGRAL UNIVERSITY

Established Under the Integral University Act 2004 (U.P. Act No.9 of 2004)
Approved by University Grant Commission
Phone No.: +91(0522) 2890812, 2890730, 3296117, 6451039, Fax No.: 0522-2890809
Kursi Road, Lucknow-226026 Uttar Pradesh (INDIA)

CERTIFICATE BY INTERNAL ADVISOR

This is to certify that **Heena Bano,** a student of **M. Tech Biotechnology** 2nd year/ 4th semester, Integral University has completed his six months dissertation work entitled **"Potential Inhibitors of Human Epidermal Growth Factor Receptor 2 using Structure-Based Virtual Screening, Docking, Molecular Dynamics Simulations and Principal Component Analysis"** successfully. She has completed this work from IIRC 7, Integral University, Lucknow under the guidance of **Dr. Mohammad Kalim Ahmad Khan**, Associate Professor in department of Bioengineering. The dissertation was a compulsory part of her **M. Tech Biotechnology.**

I wish her good luck and bright future.

Er. Adnan Ahmad
Assistant Professor
Department of Bioengineering
Faculty of Engineering

INTEGRAL UNIVERSITY

Established Under the Integral University Act 2004 (U.P. Act No.9 of 2004)
Approved by University Grant Commission
Phone No.: +91(0522) 2890812, 2890730, 3296117, 6451039, Fax No.: 0522-2890809
Kursi Road, Lucknow-226026 Uttar Pradesh (INDIA)

TO WHOM IT MAY CONCERN

This is to certify that **Heena Bano,** a student of **M. Tech Biotechnology** 2nd Year 4th semester, Integral University has completed her six months dissertation work entitled **"Potential Inhibitors of Human Epidermal Growth Factor Receptor 2 using Structure-Based Virtual Screening, Docking, Molecular Dynamics Simulations and Principal Component Analysis"** successfully. She has completed this work from IIRC 7, Integral University, Lucknow under the guidance of **Dr. Mohammad Kalim Ahmad Khan**. The dissertation was a compulsory part of his **M. Tech Biotechnology.**

I wish her good luck and bright future.

Dr. Alvina Farooqui
Head
Department of Bioengineering
Faculty of Engineering

ACKNOWLEDGEMENT

First of all, I bow in reverence to the Almighty for blessing me with strong will power, patience and confidence, which helped me in completing the present work.

At the very outset I pay my warm thanks to our Honorable **Chancellor and Founder, Integral University, Lucknow. Prof. S.W Akhtar** for providing excellent infrastructure and Lab facilities at IIRC-7 Integral University, Lucknow. I am also grateful to Honorable **Vice Chancellor Integral University, Lucknow. Prof. Javed Musarrat** for his continuous motivation and a Special vote of thanks to **Pro chancellor, Dr. Nadeem Akhtar** for his encouragement and support.

I would like to express my special thanks to **Dr. (Er.) Alvina farooqui (Head, Department of Bioengineering)** for given me an opportunity to join the department laboratory and providing all the necessary facilities ever since I started my work.

I would I like to express my deep sense of gratitude to my supervisor **Dr. Mohammad Kalim Ahmad Khan (Associate Professor),** internal advisor **Er. Adnan Ahmad (Assiatant Professor)**, and course coordinator **Dr. Salman Akhtar (Associate Professor)** for their invaluable guidance throughout the course of my dissertation work and academic session. It would have been impossible to complete this work in so short a time without her constant guidance.

I would like to thank respected dissertation coordinators **Dr. Roohi, Dr. Owais Yousuf, Er. Khwaja Osama** for their continuous support and help.

My acknowledgement will be incomplete if I do not mention **my parents and my family** with whose blessing; I was able to achieve my goal successfully. There are no words to express my feelings toward them. I silently acknowledge my debt to them.

I also like to acknowledge **Advanced Centre for Bioengineering and Bioinformatics (ACBB-IIRC-7)**, Integral University for providing facilities required for completion of my dissertation.

Date: **HEENA BANO**

LIST OF ABBREVATIONS

Abbrevation	Full form
NCBI	National Center for Biotechnology Information
PDB	Protein Data Bank
DSA	Discovery Studio Accelrys
EGF	Epidermal Growth Factor
EGFR	Epidermal Growth Factor Receptor
ER	Estrogen Receptor
ERK	Extracellular Signal-Regulated Kinase
HER-1/2/3/4	Human Epidermal Growth Factor Receptor-1/2/3/4
MAPK	Mitogen-Activated Protein Kinase
MEK	Mitogen-Activated Protein Kinase
mTOR	Mammalian target of rapamycin
PKC	Protein Kinase C
PI3K	Phosphoinositide 3-kinase
PTEN	Phosphatase and tensin homolog
RTKs	Receptor Tyrosine Kinases
RCSB	Research Collaboratory for Structural Bioinformatics
SDF	standard data format
SMARTS	SMILES arbitrary target specification
SIB	Swiss Institute of Bioinformatics
TGF-a	Transforming Growth Factor alpha
TNBC	Tripple Negative Breast Cancer
HBA	Hydrogen Bond Acceptor
HBD	Hydrogen Bond Donor
SMILES	Simplified Molecular Input Line Entry System
PR	Progesteron Receptor
LHRHa	Luteinizing Hormone-Releasing Hormone Agonist

NF-B	Nuclear Factor B
NGFs	Neuregulins
TKIs	Tyrosine Kinase Inhibitors
PSA	Polar Surface Area
MR	Molar Refractivity
RBs	Rotatable Bonds
NRs	Number of Rings
ADME	Absorption, Distribution, Metabolism, and Excretion
ADV	AutoDock Vina
ΔG	Minimum free energy of binding
MD	Molecular Dynamics
RMSD	Root Mean Square Deviation
RMSF	Root Mean Square Fluctuation
SASA	Solvent Accessible Surface Area
Rg	Radius of Gyration
BOILED	Brain Or IntestinaL EstimateD
HIA	Human Intestinal Absorption
BBB	Blood-Brain Barrier
MW	Molecular Weight
TPSA	Topological Polar Surface Area
PK	Pharmacokinetics
CYP450s	Cytochrome P450 Isozymes
PAINS	Pan Assay Interference Structure
LL	Leadlikeness
SA	Synthetic accessibility
BS	Bioavailability score
PCA	Principal Component Analysis

CONTENT

LIST OF FIGURES

LIST OF TABLES

1. INTRODUCTION

Millions to quadrillions of cells make up complex multicellular organisms, which are all evolved from a single cell, the zygote. Cell lineages tend to develop mutations over the course of an organism's lifetime as a result of numerous mutational mechanisms. While most mutations are harmless, others allow cells to escape cell cycle control, allowing them to grow and proliferate uncontrollably, eventually leading to cancer (Chatterjee N et al., 2017). Cancer is a multistage disease that requires a set of alterations for both beginning and development. Given that every cell division has the potential to generate mutations; organisms with larger bodies (more cells) and longer lifespan (more time to accumulate mutations) should be more likely to acquire cancer (Vincze O et al., 2022). Cancer cells have DNA and RNA that are very similar (but not identical) to cells from the organism from which it they came. This is why they are not always noticed by the immune system, especially when it is compromised (Sharma GN et al., 2010). Cancer is the largest cause of death in the world, with approximately 10 million death expected by 2020. The most common cancer in terms of new cases in 2020 is summarized in figure 1.1 (Aertsens, J et al., 2020).

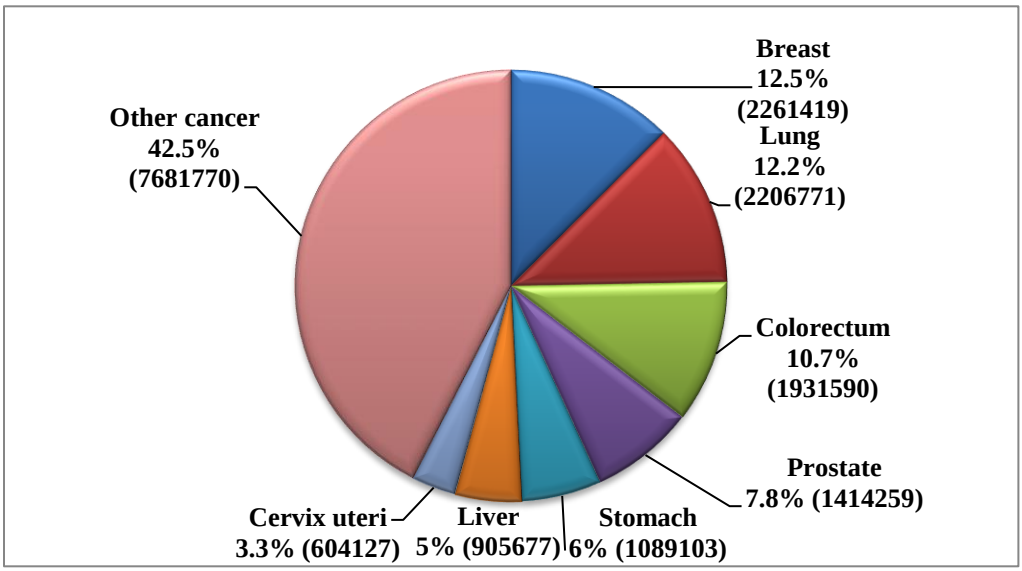

Figure 1.1: Estimated no. of new cases in 2020, worldwide, both sexes, all ages (excl. NMSC)

The worldwide burden of cancer is continuing to rise, owing to the ageing and growing of the global population, as well as an increase in the consumption of cancer-causing habits, especially smoking, mainly in economically developing nations. In terms of cancer, India is diverse. Local cultural factors and lifestyle choices may have played a role in the variability and variances in cancer incidence patterns in India (Gupta S et al., 2021). Among them breast cancer is the most common cancer among women in India and other poor nations (Labani S et al., 2020, Bhat V et al., 2019, Aertsens, J et al., 2021). Breast cancer will affect 2.3 million women globally in 2020, with 685 000 fatalities. Breast cancer had been diagnosed in 7.8 million women in the previous 5 years as of the end of 2020, making it the most common cancer in the world. Breast cancer refers to the rapid development and multiplication of cells that begin in the breast tissue, and is usually termed after the body part in which it first appeared. There are two types of tissues in the breast: glandular tissues and stromal (supporting) tissues. The milk-producing glands (lobules) and ducts (milk passageways) are housed in glandular tissues, while the fatty and fibrous connective tissues of the breast are found in stromal tissues. Lymphatic tissue- immune system tissue that drains cellular fluids and waste is also found in the breast (Khuwaja GA et al., 2004).

The heterogeneity of breast cancer has long been recognized and studied. Breast cancers have been classified on the basis of estrogen receptor expression and later on the basis of HER2 (Nounou MI et al., 2015), following an initial classification based on histological features in the 1980s. The microarray revolution had proven that phenotypic variations across breast tumors were a reflection of their mRNA expression profiles by the year 2000. The more recent genetic revolution has proven this. Breast cancer molecular subtypes were discovered using DNA microarrays, and they included Luminal A (ER+, PR+, and HER2-), Luminal B(ER+, PR-, and HER2 -), HER- 2 positive (ER-, PR-, and HER2+) and triple negative breast cancer (ER-, PR-, and HER2-) (Weigelt B et al., 2010, Vuong D et al., 2014, Fukada I et al., 2018, Anurag M et al., 2020, Hashmi AA 2018, https://www.mayoclinic.org/diseases-conditions/breast-cancer/in-depth/breast-cancer/art-20045654).

Human epidermal growth factor receptor-2 (HER2) is a member of the epidermal growth factor receptor (EGFR) family with a molecular mass of 185 kDa and overexpressed in breast cancer. The EGFR family consists of four closely related receptors: HER1, HER2, HER3 and HER4. These receptors all include three domains: an extracellular domain which is similar

among the four receptors, a short transmembrane region and an intracellular tyrosine kinase domain. The extracellular domain has four sub-domains (Dong Y et al., 2019). Amplification of the HER2 gene in breast cancer is linked to tumor cell multiplication and invasion, which leads to localised progression and distant metastases. Signal transduction mediated by the activation of the PI3K (phosphoinositide-3-kinase)/AKT (Protein kinase B) and Ras/Raf/MEK/MAPK (Mitogen Activated Protein Kinases) pathways is related with the proliferation and development of some aggressive breast cells, resulting in undesirable biological features and clinical consequences (Turke Abet al., 2012). Cancer cells with an excess of copies of the HER2 gene (HER2-positive tumors) produce an excessive amount of the growth-promoting protein HER2 (https://www.mayoclinic.org/diseases-conditions/breast-cancer/in-depth/breast-cancer/art-20045654). Because HER-2 lacks a recognized ligand, it must rely on heterodimerization with other HER receptors or homodimerization with itself when expressed at very high levels on the cell surface to be activated. Over expression of HER-2 is linked to aberrant signalling (proliferation, survival, differentiation, angiogenesis, invasion, and metastasis), and eventually tumor formation Figure 1.2 (Aziz SW et al., 2013).

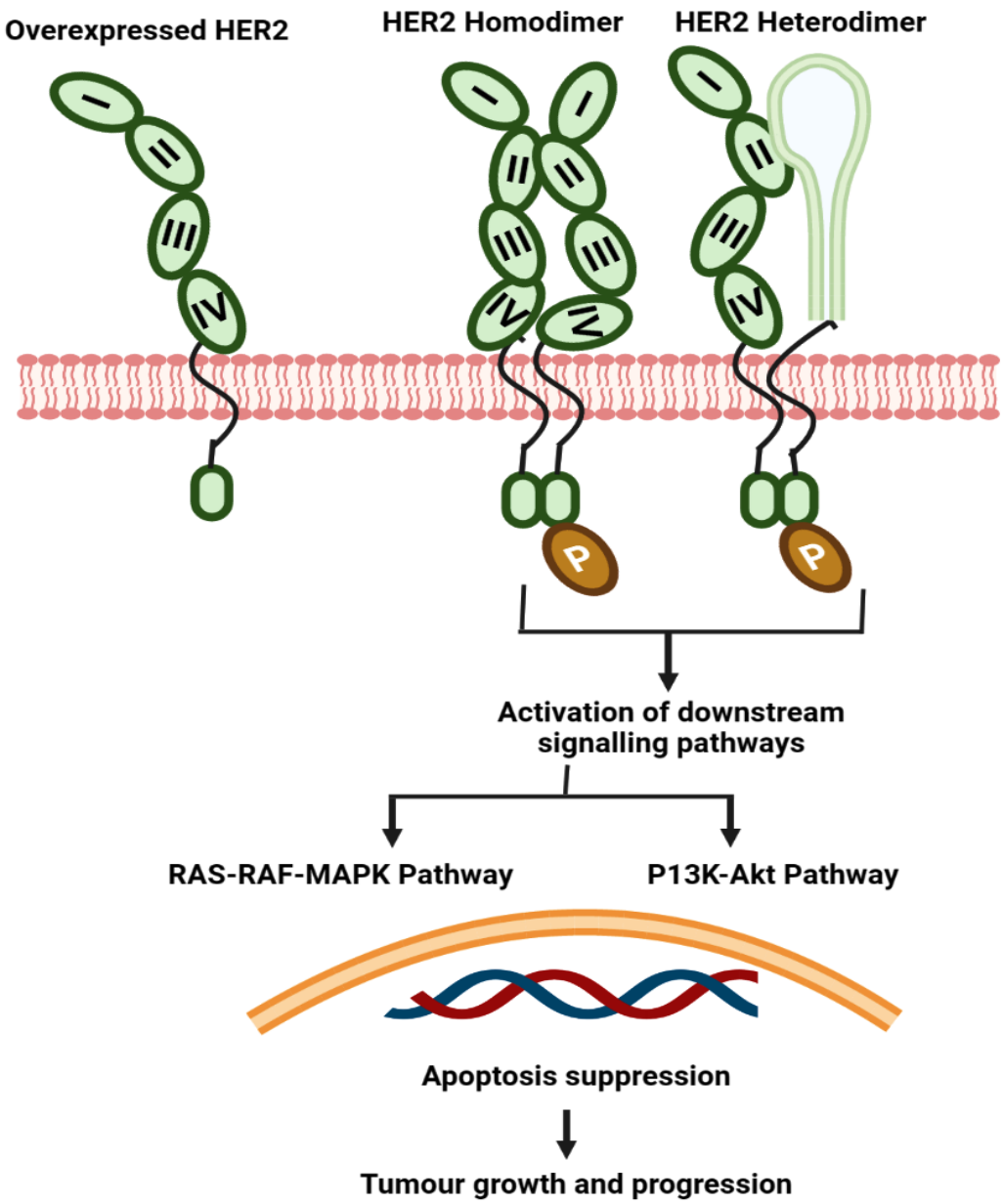

Figure 1.2: Highly diversified oncogenic signaling of HER2 in HER2-positive BC cells.

Current clinical treatment of early stage HER2+ breast cancer mainly relies on monoclonal antibodies and tyrosine kinase inhibitors (Pernas, S et al., 2018). For example, monoclonal antibody pertuzumab binds the extracellular sub-domain II, blocking the dimerization of HER2 with other EGFR family members such as HER3 and thereby inhibiting the downstream signaling pathways. While tyrosine kinase inhibitors, such as, lapatinib and neratinib, bind the intracellular domain, suppressing the autophosphorylation of tyrosine and

leading to growth inhibition of HER2+ cancer cells. Besides, a nucleic acid aptamer that binds the extracellular domain and a peptidomimetic that binds the extracellular sub domain IV of HER2 have been demonstrated to be able to inhibit the signaling pathways, providing new possibilities for the therapy of HER2+ breast cancer (Dong et al., 2019). The present study aims to identify potential HER2 inhibitors from MCULE libraries (https://mcule.com/) consisting of more than five million investigational compounds using SBVS, drug-likeness filtration, ADMET profiling, multi scoring molecular docking, and MD simulation of 100ns duration. Since KIFC1 plays many roles in driving tumour progression and development, inhibiting it through new small lead molecules will undoubtedly benefit cancer prevention and treatment.

2. REVIEW OF LITERATURE

Breast cancer dates back to approximately 1,500 years B.C. More than 3,500 years ago, the disease was first reported by the ancient Egyptians. Hippocrates, the father of Western medicine, described breast cancer as a humoral disease in 460 B.C. Hippocrates was the first to define the term karkinos, which is a Greek word for crab or cancer. Following that, in 200 A.D., Galen, who detailed the categorization of abnormal growths, wrote a treatise titled "On Tumors against Nature." Galen believed that cancer could appear anywhere in the body, but he had seen it more frequently in the breasts of women whose menstruation was either abnormal or inconsistent (Nounou et al., 2015).

Prevalence of breast cancer among females:

Cancer claimed the lives of approximately 10 million people worldwide in 2020, and this figure has risen dramatically in recent years, wreaking havoc on the socioeconomic landscape, particularly in low-and middle-income countries. In 2020, breast cancer will be the leading cause of new cases, followed by lung cancer, colon and rectal cancer, prostate cancer, skin cancer, and stomach cancer (Figure 1.1). In 2020, lung cancer patients had the highest death rates, followed by colon and rectum, liver, stomach, and breast cancer patients (Ryzhov et al., 2022).

Breast cancer in men:

Male breast cancer is a rare tumour throughout the world. Men account for about 1% of all breast cancer cases. On the other hand, breast cancer in men is more frequently hormone receptor positive and may be more sensitive to hormonal therapy. BRCA2 gene mutations appear to be more dangerous than BRCA1 gene mutations. Men are diagnosed at an older age and at a later stage of the disease than women. Male breast cancers are more likely to express estrogen and progesterone receptors (PRs) and less likely to overexpress Her-2/neu than female breast cancers. The most common presentation is a lump or nipple inversion, but it is frequently diagnosed late, with more than 40% of individuals diagnosed at stage III or IV disease. The majority of tumours are ductal, and 10% are ductal carcinoma in situ. National initiatives to provide information and support to male breast cancer patients are becoming increasingly important (Shah et al., 2020).

Types of Breast Cancer

Luminal A:

Luminal A is the most common molecular subtype, accounting for 40% to 50% of all invasive breast tumours. Luminal A tumours are frequently low-grade, with the best prognosis of the intrinsic subtypes (Vuong D et al., 2014). At the St. Gallen International Breast Cancer Conference in 2013, breast cancers that were positive for one or both estrogen receptor (ER) and progesterone receptor (PR), negative for HER2, and had a low Ki-67 labelling index were designated as luminal A type tumours (Fukada I et al., 2013).

Luminal B:

The Luminal B subtype accounts for approximately 40% of node-negative early-stage breast tumours, necessitating additional research to find new treatments (Anurag M et al., 2020). Luminal B cancers were more severe and had a worse prognosis than luminal A cancers (Vuong et al., 2012). Luminal B tumours were significantly more common in younger age groups than luminal A tumours (Hashmi AA et al., 2018). These cancers are ER-positive, PR-negative, and HER2-positive. Chemotherapy, hormone therapy, and HER2-targeted therapy are likely to benefit Luminal B breast cancers (https://www.mayoclinic.org/diseases-conditions/breast-cancer/in-depth/breast-cancer/art-20045654).

Basal like:

These tumours are also known as triple negative because they lack the protein expression of ER, PR, and HER2. According to gene expression analysis, the basal-like subtype accounts for approximately 75% of triple-negative breast tumours. Triple negative breast cancers have a worse prognosis than other molecular subtypes because therapy breakthroughs have lagged behind. Premenopausal women and those with a BRCA1 gene mutation are more likely than white women in the United States to develop these cancers (Street W et al., 2019). They are also more prevalent in premenopausal women and those who have a BRCA1 gene mutation. TNBC patients had high p53 expression, lymphocytic infiltration, and multimodality (Gonçalves Jr H et al., 2018). They were treated with extensive surgery and chemotherapy.

HER- 2 Positive:

HER-2 (human epidermal growth factor receptor 2), also known as c-ErbB2/c-neu, is found in 15-20% of breast tumours worldwide (Loibl S et al., 2017, Arteaga CL et al., 2012). Previous research has shown that HER2 is an effective therapeutic target for the treatment of breast cancer. The HER2 oncogene has been linked to the progression and growth of breast cancer. The HER-2 oncogenes are found on chromosome 17. The primary function of the HER2 oncogene is to encode the transmembrane receptor tyrosine kinase (Wang J et al., 2019). This category includes tumours that are ER and PR negative but HER2 positive (https://www.mayoclinic.org/diseases-conditions/breast-cancer/in-depth/breast-cancer/art-20045654).

Symptoms of breast cancer:

Early signs of breast cancer include a lump or thickened tissue in the breast (Hermansyah D, et al., 2022). An early breast cancer diagnosis increases the chances of recovery. Another sign is breast or armpit pain that does not vary with the monthly cycle.

- Breast skin that piles up or turns redder than an orange's skin.
- A rash on or near one of the nipples.
- Nipple discharge with blood
- An inverted or sunken nipple
- Changes in breast size or shape
- Skin peeling, flaking, or scaling on the breast or nipple
- Even though most bumps are not cancerous, women should have them checked by a doctor (Russo et al., 1980).

Genetics of Breast Cancer:

"BRCA" is an abbreviation for "BReast CAncer gene." The BRCA1 and BRCA2 genes have been discovered to influence a person's risk of developing breast cancer. Every person carries the BRCA1 and BRCA2 genes. Contrary to popular belief, the BRCA genes do not cause breast cancer. In reality, these genes have a significant impact on breast cancer prevention. They aid in the repair of DNA damage that can lead to cancer and the uncontrolled spread of malignancies. As a result, the BRCA genes are known as tumour suppressor genes.

These tumour suppression genes, however, do not work properly in some people. When a BRCA gene is altered, it may lose its ability to repair damaged DNA and help prevent breast cancer. As a result, people who have a BRCA gene mutation are more likely to develop breast cancer and to develop it at a younger age. A gene mutation can also be passed down through generations by the person who carries the mutant gene (Effiong et al., 2022).

Stages of breast cancer:

The stage of cancer is determined by the size of the tumour and whether it has spread to the lymph nodes or other parts of the body. Breast cancer can be staged in several ways. Steps 0 to 4, which can be further sub divided :

Stage 0: Ductal carcinoma in situ (DCIS), in which the cells are contained within the duct and have not spread to the surrounding tissues.

Stage 1: At the start of this stage, the tumour is up to 2 cm across and has not spread to any lymph nodes.

Stage 2: The tumour has grown to 2 cm in diameter and has begun to spread to nearby lymph nodes.

Stage 3: The tumour has grown to be up to 5 cm in diameter and has spread to a few lymph nodes.

Stage 4: Stage 4 means that the cancer has spread to other organs, such as the bones, liver, brain, or lungs (Effiong et al., 2022).

Risk factors:

The precise cause is unknown, but certain risk factors make it more likely. Some of these are avoidable.

Age: The risk grows with age. Breast cancer has a 0.6 percent chance of developing within the next decade if you are 20 years old. This figure rises to 3.84 percent by the age of 70.

Breast cancer or breast lumps: women who have previously had breast cancer are more likely than those who have never had it to develop it again. Having benign or non-cancerous breast lumps increases the risk of developing cancer later in life. Atypical ductal hyperplasia and lobular carcinoma in situ are two examples. (Eltayeb et al., 2014).

Dense breast tissue: Breast cancer is more likely to develop in breast tissue with a higher density.

Estrogen exposure and breast-feeding: Longer exposure to estrogen appears to increase the risk of breast cancer. This could be due to periods starting earlier or entering menopause later than usual. Estrogen levels are higher between these times. Breast feeding appears to reduce the risk of developing breast cancer, possibly because pregnancy followed by breastfeeding reduces estrogen exposure.

Body weight: Women who are overweight or obese after menopause may be at a greater risk of developing breast cancer, possibly due to enhanced estrogen levels. High carbohydrate consumption could also play a role.

Alcohol consumption: It appears that a higher rate of regular alcohol consumption plays a role. According to research, women who consume more than three drinks per day are 1.5 times more likely to develop breast cancer (Tarar et al., 2018).

Radiation exposure: Radiation treatment for a cancer that is not breast cancer raises the risk of developing breast cancer later in life.

Hormone treatments: Hormone replacement therapy (HRT) and oral birth control pills have been linked to breast cancer due to elevated estrogen levels.

Causes of Breast Cancer:

A woman's breast after puberty is made up of fat, connective tissues, and thousands of lobules, which are tiny glands that produce milk for breast-feeding. Milk is carried to the nipples via tiny tubes called ducts. Cancer causes the body's cells to multiply uncontrollably. Cancer is caused by abnormal cell growth. Breast cancer typically begins in the inner lining of milk ducts or lobules that supply milk to them. It can then spread to other parts of the body. (Rehm J et al., 2007).

Diagnosis: A diagnosis is frequently made as a result of routine screening or when a woman consults her doctor after noticing symptoms.

Some diagnostic tests and procedures aid in the confirmation of a diagnosis.

Breast exam: The doctor will examine the patient's breasts for lumps and other symptoms. The patient will be asked to sit or stand in various positions with her arms, such as above her head and by her sides.

Imaging tests: Mammography is a category of x-ray that is commonly used for early breast cancer detection. It generates images that can aid in the detection of lumps or abnormalities. A suspicious result can be followed by further investigation. However, mammography can occasionally detect a suspicious area that is not cancerous. This can result in unnecessary stress and, in some cases, interventions. An ultrasound scan can help determine whether a mass is solid or fluid-filled. An MRI scan involves injecting a dye into the patient to determine the extent of the cancer's spread.

Biopsy: A tissue sample is surgically removed for laboratory analysis. This can reveal whether the cells are cancerous and, if so, what type of cancer they are, as well as whether the cancer is hormone-sensitive.

Lumpectomy: Trying to remove the cancerous cells as well as a small margin of healthy tissue around them can help prevent cancer spread. If the tumour is small and easily separated from the surrounding tissues, this may be an option.

Mastectomy: The lobules, ducts, fatty tissues, nipples, areola, and some skin are removed during a simple mastectomy. Radical mastectomy involves the removal of muscle from the chest wall as well as lymph nodes in the armpit.

Sentinel node biopsy: Because breast cancer can spread through the lymphatic system into other parts of the body, removing one lymph node can prevent it from spreading.

Auxiliary lymph node dissection: If cancer cells are found on a node called the sentinel node, the surgeon may recommend removing several nymph nodes in the armpit to prevent disease spread.

Reconstruction: Reconstruction after breast surgery can recreate the breast so that it resembles the other breast. This can be done concurrently with or after a mastectomy. A breast implant or tissues from another part of the patient's body may be used by the surgeon.

Radiation therapy: To destroy cancer cells, controlled doses of radiation are directed at the tumour. It can kill any remaining cancer cells when used with chemotherapy about a month after surgery. Each session lasts a few minutes, and depending on the goal and extent of the cancer, the patient may require three to five sessions per week for three to six weeks. The type of breast cancer will determine which type of radiation therapy, if any, is best. For patients who are unable to undergo surgery, chemotherapy, or radiotherapy, it may be their only option. The effect usually lasts up to five years after surgery. The treatment will have no effect on cancer that is not hormone sensitive. Tamoxifen, aromatase inhibitors, and ovarian ablation or suppression are some examples. Goserelin, a luteinizing hormone-releasing hormone agonist (LHRHa) drug, is used to suppress the ovaries (J. Russo and H. Russo et al., 1980). Hormone therapy may have an impact on a woman's fertility in the future.

Biological treatment: Specific types of breast cancer are eradicated by targeted drugs. Trastuzumab (Herceptin), lapatinib (Tykerb), and bevacizumab are a few examples (A vastin). All of these drugs serve different functions (Effiong et al., 2002).Treatment will be determined by the following factors: the type of breast

The main option include: Radiation therapy, surgery, biological therapy or targeted drug therapy, hormone therapy, and chemotherapy are some of the treatments available. The stage of the cancer, other medical conditions, and individual preference will all influence thedecision. If surgery is required, the option will be determined by the diagnosis and the individual. Fatigue, lymphedema, darkening of the breast skin, and irritation of the breast skin are all side effects.

Chemotherapy: If there is a high risk of recurrence or spread, cytotoxic drugs may be used to kill cancer cells. This is known as adjuvant chemotherapy. If the tumour is large, chemotherapy may be given prior to surgery to shrink it and make removal easier. This is referred to as neo-adjuvant chemotherapy. Chemotherapy can also be used to treat cancer that has spread to other parts of the body, and it can alleviate some symptoms, particularly in the later stages. It could be used to reduce estrogen production, which can promote the growth of some breast cancers. Nausea, vomiting, loss of appetite, fatigue, sore mouth, hair loss, and a

slightly increased susceptibility to infections are among the side effects. Many of these can be controlled with medications (Ye et al., 2002).

Hormone blocking therapy: In hormone-sensitive breast cancers, hormone blocking therapy is used to prevent recurrence. These are known as estrogen receptor (ER) and progesterone receptor (PR) positive cancers. Hormone blocking therapy is typically used after surgery, but it can also be used before surgery to shrink the tumour.

Cell Death Pathways

Cell death is required for an organism's growth, development, senescence, and death (Liu et al., 2018). It can happen through a variety of regulatory mechanisms, such as apoptosis, necrosis, necroptosis, pyroptosis, and ferroptosis (Ruoxi Z et al., 2021). Apoptosis and autophagy are types I and II of programmed cell death. In tumour cells, autophagy is a double-edged sword. It has the ability to degrade and recycle cellular components in an orderly manner in order to maintain homeostasis and promote tumour cell survival. Excessive autophagy, on the other hand, can result in autophagic cell death (Yu et al., 2008). Apoptosis, in contrast to autophagy, has been identified as a highly regulated and controlled process that promotes tumour cell death.

Apoptosis is a type of cellular suicide that is initiated by either extracellular (extrinsic apoptosis) or intracellular (intrinsic apoptosis) signals. Cell contraction, nuclear fragmentation, chromatin aggregation, DNA fragmentation, mRNA decay, and the formation of apoptotic bodies are some of its biochemical characteristics (Roos and Kaina et al., 2013). Excessive apoptosis causes atrophy, whereas insufficient apoptosis causes uncontrolled cell proliferation, as seen in tumours. To maintain cell homeostasis, normal breast cells maintain a balance of cell proliferation and apoptosis, anti apoptosis, and pro apoptosis. When the balance is upset, activated anti apoptotic signal pathways or a lack of pro apoptotic signal pathways can result in uncontrolled cell proliferation, therapeutic resistance, and cancer cell recurrence (Mohammad et al., 2015). Multiple factors, such as growth factors, DNA damage, reactive oxygen species (ROS), and UV radiation, can promote uncontrolled cell growth in BC cells via mitochondrial, FasL/Fas-, PI3K/AKT-, ROS-, nuclear factor B (NF-B)-, and MAPK-mediated pathways, disrupting the balance of pro apoptotic and anti apoptotic effects.

Targeting apoptotic pathways is thus an effective strategy for identifying candidate drugs derived from natural products for the treatment of BC (Rajabi et al., 2021).

PI3K/AKT Pathway Mediated Apoptosis

The PI3K/AKT pathway is activated by ligands such as insulin, growth factors, and hormones. When PI3K is activated, it phosphorylates AKT, and activated AKT regulates Bad, a proapoptotic member of the Bcl-2 family, to inhibit mitochondrial-mediated apoptosis. Alternatively, activated AKT phosphorylates other components involved in cell growth, such as the mTOR complex and IkB/NF-B (Miricescu et al., 2020). As a result, inhibiting the PI3K/AKT pathway can promote cell apoptosis.

MAPK Pathway–Mediated Apoptosis

Three protein kinases phosphorylate and activate MAPK pathways in a sequential manner: MAPKKK activates MAPKK, which then activates MAPK. In mammalian cells, MAPKs are traditionally classified as ERK, JNK, and p38 kinase. MAPKs can transmit extracellular and intracellular signals via cascade reactions to regulate cell growth, proliferation, differentiation, migration, and apoptosis.

MAPKs appear to be important targets in natural product-induced BC cell apoptosis, according to mounting evidence. Chen and Sun discovered in 2012 that formononetin increased the Bax/Bcl-2 ratio in MCF-7 cells by activating the Ras-p38MAPK signalling pathway, resulting in cell apoptosis (Chen and Sun et al., 2012). According to Kim et al., genipin, a constituent of Gardenia jasminoides J. Ellis, activated p38 and JNK signals to downregulate Bcl-2 and upregulate Bax and cleave caspase-3, implying that genipin induced MDA-MB-231 cell apoptosis via the MAPK pathway. Deoxypodophyllotoxin (DTP) is a plant extract derived from Juniperus communis L.(Benzina et al.,2015) that DTP can induce BC cell apoptosis by inhibiting the ERK and NF-B signalling pathways (Fan et al., 2015). proposed in 2015 that emodin inhibited MCF-7 cell proliferation, and subsequent research revealed that emodin promoted MCF-7 cell apoptosis by activating the JNK-AP1 signal transduction pathway.

JAK-STAT3–Mediated Apoptosis

JAK/STAT signalling can convert an extracellular signal into a transcriptional response that helps cancer progress and spread. Extracellular signals such as IL-6, EGF, interferon, and others can stimulate JAK2 and STAT3 activation. Phosphorylated STAT3 then enters the nucleus, where dimerized STAT3 can activate or inhibit transcription of target genes such as BclXL, p21, and Myc to regulate cell apoptosis.

In the case of natural products, inhibiting the JAK/STAT3 pathway may be a viable strategy for inducing BC cell apoptosis. Apigenin, according to Xu et al. (2014), can induce MDA-MB-453 cell apoptosis by up regulating cleaved caspase-8/3 and PARP, inhibiting JAK2 and STAT3 activation (phosphorylation), and decreasing STAT3 nuclear tillering (Seo et al., 2014).

Human Epidermal Growth Factor (HER) Family of Receptors

The HER receptor family is made up of four RTKs with similar homology: HER1 (also known as epidermal growth factor receptor or EGFR), HER2, HER3, and HER4. Ligand binding causes either homodimerization of like receptors or heterodimerization of different receptors. HER2 is classified as an "orphan receptor" because it lacks a known ligand and preferentially collaborates with other members of the family to enhance ligand-induced signalling. In HER2 overexpressing preclinical models, ligand-independent formation of HER2 homodimers has also been demonstrated. HER2 overexpression occurs in 20–30% of breast cancer patients and is associated with a poor prognosis and decreased survival (Demonty et al., 2007). Other members of the HER receptor family are also potential targets for breast cancer treatment. For example, EGFR-specific small-molecule tyrosine kinase inhibitors induce the formation of inactive HER1/HER2 heterodimers in cell lines that coexpress HER2 and HER1/EGFR (Moulder et al., 2001). Thus, HER1/EGFR inhibitors can prevent HER2 from interacting with other signalling partners such as HER3 and HER4.

Ligands of HER receptors

Understanding the action of HER receptor ligands is critical to understanding the role of the receptors themselves. HER receptors are found as monomers. However, upon ligand binding, they form receptor dimers, which can be homodimers of the same receptor type (e.g., HER1-HER1) or heterodimers of different receptor types (e.g., HER1-HER2) (Kovacs et al., 2022).

Dimer formation is driven by the higher stability of the complex formed between a ligand and two receptors. The HER1 receptor serves many functions and is activated by six ligands: EGF, TGFa, amphiregulin, heparin-binding EGF-like growth factor, betacellulin, and epiregulin. Neuregulins (NGFs), a family of structurally diverse peptides, are bound by HER3 and HER4 receptors. All neuregulins signal via mitogen activated protein kinase (MAPK) (Ghauri et al., 2022).

HER2 is a co-receptor for a variety of ligands, and it is frequently transactivated by EGF-like ligands, resulting in the formation of HER1-HER2 heterodimers. Neuregulins can cause HER2-HER3 and HER2-HER4 heterodimers to form. No known ligand, however, can promote the HER2 homodimer (HER2-HER2), implying that no existing ligand binds directly to HER2. Analysis of representative pox virus growth factors, viral HER ligands, revealed that none bind directly to HER2, but all are capable of recruiting HER2 into heterodimers. This finding led us to believe that HER2 acts as a ligand-free receptor for many, if not all, HER ligands. Interactions between HER receptors are not at random. Instead, there is a distinct hierarchy that prefers HER2 as an interaction partner (Bremer A et al., 2022).

Mechanisms of actions of HER2 inhibitors

The HER2 inhibitors developed for the treatment of HER2-positive breast cancer fall into three categories: 1) Trastuzumab and pertuzumab monoclonal antibodies, 2) antibody drug conjugates (T-DM1 and DS-8201a), and 3) tyrosine kinase inhibitors (TKIs) (lapatinib, neratinib, and tucatinib). As previously discussed, phospho-tyrosine residues in RTK kinase domains and C-terminal tails serve as docking sites for various signalling proteins, resulting in activation of various signalling pathways. TKIs work by inhibiting RTK auto- and trans-phosphorylation, which prevents oncogenic signaling. Lapatinib is a dual TKI that inhibits both HER2 and EGFR tyrosine kinase activities (Davis et al., 2011). It is a reversible TKI that competes for the ATP binding site in the kinase domains with ATP. On the other hand, lapatinib upregulates HER3 and induces HER2-HER3 dimerization, which promotes proliferation while limiting its own antitumor activity. Neratinib is a pan-HER TKI that inhibits all HER family members' tyrosine kinase activities (Fig. 1). (Davis et al., 2011). It is an irreversible TKI that binds to a specific cysteine residue (Cys-773 or Cys-805) in the RTKs' ATP-binding pocket. The toxicity of neratinib is significant and dose-limiting. More

than 40% of Neratinib-treated patients have grade 3–4 diarrhoea, compared to 2% in the control group. In contrast, only 6% of patients receiving lapatinib experience grade 3 diarrhoea, with no grade 4 diarrhoea. Tucatinib, which is less toxic than neratinib, is a reversible HER2-specific TKI that competes with ATP for the ATP-binding site in the kinase domain (Fig 2.1). For example, 12.9 percent of patients receiving a combination treatment regimen with or without tucatinib experience grade 3 diarrhoea (Murthy et al., 2020). Neratinib and tucatinib are relatively new drugs, having received FDA approval in 2017 and 2020, respectively, and their potential off-target effects are unknown.

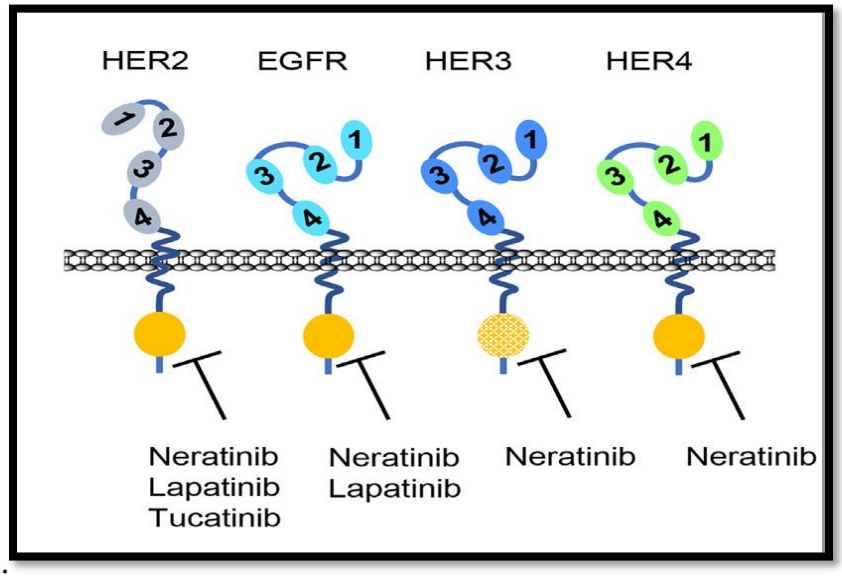

Figure 2.1. Inhibition of tyrosine kinase activities of HER family members by lapatinib, neratinib and tucatinib. The hatched oval in HER3 indicates that its tyrosine kinase is severely impaired (Zhang et al., 2021)

Role of HER2 in drug-resistant HER2-positive BC

PEPDG278D's potent inhibitory activity against drug-resistant HER2-positive breast cancer suggests that HER2 remains an important oncogenic driver in HER2-positive breast cancer resistant to current HER2 inhibitors. The PEPDG278D findings suggest that HER2 depletion may be the most effective HER2-targeting strategy in HER2-positive breast cancer. This notion is consistent with the notion that HER2 depletion may be most effective in disrupting the vast oncogenic signalling network orchestrated by overexpressed HER2, including disruption of its homo- and heterodimeric signalling units, reduction of p95HER2, and

elimination of nuclear and mitochondrial HER2 (Fig. 2.1). Currently available HER2 inhibitors have little or no effect on HER2 levels. According to the PEPDG278D findings, other molecular changes linked to drug resistance, such as p95HER2, PIK3CA mutation, PTEN loss, SRC activation, and Cyclin E overexpression, may not sustain HER2-positive BC cells if HER2 is depleted, according to the PEPDG278D findings. A systemically delivered trastuzumab-conjugated nano-construct carrying HER2 siRNA significantly inhibits the growth of trastuzumab-resistant tumours in mice. Furthermore, disrupting the HER2-CB2R heteromers inhibits trastuzumab-resistant HER2-positive cells in vitro and in vivo. PEPDG278D's ability to induce HER2 and EGFR depletion is especially promising, given that EGFR is overexpressed in approximately 35% of HER2-positive BC tumours and is associated with poor prognosis. Indeed, siRNA-mediated EGFR knockdown inhibits the growth of trastuzumab-resistant HER2-positive BC cells (Zhang Y et al., 2021).

AIM AND OBJECTIVES

Suppression of HER2 protein by small molecules is a lucrative strategy to prevent the uncontrolled growth of cancerous cells. The proposed study aims to investigate small molecule inhibitors targeting HER2.

To accomplish the aim following objectives were proposed.

1. Structure-Based Virtual Screening (SBVS) using the MCULE drug discovery platform.
2. Molecular Docking of SBVS-hits using AutoDock Vina (ADV).
3. Toxicity filtration using SMILES arbitrary target specification (SMARTS) algorithm.
4. ADME (Physiochemical, Lipophilicity, Solubility, Pharmacokinetics, Drug-likeness, Medicinal chemistry attributes) profiling of toxicity-succeeded ligands.
5. MD simulation (10 ns) and Principal Component Analysis of the top two hits and comparison with reference drug (tucatinib) of HER2.

3. MATERIALS AND METHODS

HER2 protein retrieval and optimization

3D crystal structure (2.25 Å) of the motor domain of human HER2 was retrieved from research collaboratory for structural bioinformatics (RCSB) protein data bank (PDB). The only apoprotein was taken to prepare a 3D input file suitable to adopted docking tools by removing undesired heteroatoms, ions, and molecules, e.g., adenosine-5'-diphosphate, Mg+2, and H2O. The CHARMm force field was assigned to optimize and minimize 3D structure. The PropKa utility tool was used to keep protonation states of protein at pH 7.4 (Morris G. M et al., 1998, Morris G.M et al., 1996, Khan F.I et al., 2020, Umar A. M et al., 2021, Bas D.C et al., 2008).

Structure-based virtual screening

The MCULE, an interactive drug discovery portal, was used for high-throughput SBVS of small molecules from its library containing over a hundred million synthetically accessible ligand molecules. A systematic query was set in the SBVS input search box. Lipinski rule of five (RO5: MW ≤ 500 Da; HBD ≤ 5; HBA ≤ 10; LogP ≤ 5), polar surface area (PSA: 140 $Å^2$), molar refractivity (40 ≤ MR ≤ 130), rotatable bonds (RBs) ≤ 10, N and O atoms <=10, and number of rings (NRs) ≤ 7 filtrations were considered in the mcule's SBVS workflow. Sample size, diversity selection, and similarity search cutoff value for the query string were respectively taken 1000, 100, and 0.85. The open babel linear fingerprint search algorithm was employed to execute the SBVS run as an advanced option. The remaining search parameters were assigned default values of the SBVS workflow (Kiss R et al., 2008, Shakil S et al., 2019).

3D structure retrieval and optimization of HER2 inhibitors

2D structure of known inhibitors viz., Lapatinib (CID: 208908), Neratinib (9915743), and Tucatinib (51039094) in standard data format (SDF) were accessed from PubChem database (Wu J et al., 2014, Watts C.A., 2013, Zhang W., 2016).Conversion of SDF-2D to PDB-3D was completed using the BIOVIA discovery studio visualizer. All selected inhibitors were energetically optimized and minimized using the same protocol as HER2 protein.

Toxicity filtration

The toxicity checker facility of MCULE was used to examine the presence of substructure, scaffolds, or moieties, also referred to as toxicophores found in chemicals that are profoundly correlated with unwanted properties commonly associated with human and environmental toxicity. Toxicity Checker uses the robust SMARTS (SMILES arbitrary target specification) toxic matching rules. SMARTS is an extension of SMILES, an acronym of Simplified Molecular Input Line Entry System used to represent the computer-ready chemical structure of molecules (Kiss R et al., 2014).

Absorption, distribution, metabolism, and excretion profiling

At the early stage of the drug discovery process, moving with ADME satisfied compounds is imperative to find desired results in wet-lab experiments. Toxicity sifted ligands was assessed on various ADME parameters, including physicochemical properties, lipophilicity, pharmacokinetics, drug-likeness and medicinal chemistry attributes using the SwissADME web tool (Zhang W et al., 2016).

Computational docking

AutoDock Vina incorporated to MCULE drug discovery platform (https://mcule.com/), DockThor tool of DockThor-virtual screening web server (https://dockthor.lncc.br/v2/), and SwissDock of Swiss Institute of Bioinformatics (SIB) (http://www.swissdock.ch/) were used for molecular interaction studies between HER2 and SBVS-hits. The mean of ΔG terms exhibited by selected docking tools was intended to get consensus docking hits.

AutoDock Vina

The dock-prepared PDB structure of HER2 was imported to the AutoDock Vina (ADV) interface. A grid size of 40 Å in each x, y, and z axes of AutoGrid setup was drawn to cover the protein binding site area. The grid box covering the protein binding center was drawn with variable grid points in x (12.2935 Å), y (24.3815 Å), and z (34.9715 Å) axes. ADV parameters for the maximum number of binding modes per ligands and exhaustiveness were taken as the default, i.e., 2 and 1. Minimum free energy of binding (ΔG) was chosen as a selective parameter to find one of the best binding affinities and pose for each of the ligand molecule docked into the active site of HER2 (OLEG TROTT A. J. O et al., 2010, Ajijur R et

al., 2021, Khan M. K. A., 2018, Ahmad K. M. K 2020, Khan, M. K. A et al., 20118, Khan M. K. A et al., 2020).

Molecular dynamic simulation

MD simulation was performed on docked complexes of HER2 with top two ligand hits viz., Mcule-9083675198-0-12 and Mcule-2082061687-0-14, and known inhibitor Tucatinib at 300K at the MM level using GROMACS 5.1.2 (Zoete V et al., 2010).The ligands were extracted from the docked complexes utilizing the gmx grep module. The CGENFF server obtained the topology and forcefield parameter files of the ligand. The topologies were generated for HER2 utilizing pdb2gmx modules of gromacs, Mcule-9083675198-0-12 Mcule-2082061687-0-14, and Tucatinib using the CGENFF server were merged (Van Der Spoel D., 2005, Vanommeslaeghe K., 2012).

All docked complexes were soaked in a dodecahedron box of water molecules with a margin of 10 Å. The gmx editconf module was used for creating boundary conditions. The charges on the docked complexes were neutralized by adding Na^+ and Cl^- ions using the gmx genion module to maintain neutrality, preserving the physiological concentration of 0.15 M. The system was then minimized for 25,000,000 steps using the steepest descent algorithm. Finally, the system temperature was raised from 0-300K during their equilibration of 100 ps duration at constant NVT and NPT. After the equilibration phase, the particle mesh was applied following the Ewald method (Vanommeslaeghe K et al., 2010, Petersen H. G et al., 1995). Finally, the protein-ligand system was introduced to the 10 ns of MD simulation performed under identical conditions at 1 bar and temperature of 300K. The gmx rms, gmx rmsf, and gmx sasa, gmx ΔGsolv, gmx Rg, and gmx HB modules of GROMACS were used to get the root mean square deviation (RMSD), root mean square fluctuation (RMSF), solvent accessible surface area (SASA), free energy of solvation (ΔGsolv), and radius of gyration (Rg) plots (Zoete V et al., 2010, Van Der Spoel D et al., 2005, Vanommeslaeghe K et al., 2012, Vanommeslaeghe K et al., 2010, Petersen H. G., 1995, Stenberg S et al., 2020)

4. RESULTS AND DISCUSSION

Structure-based virtual screening

SBVS approach was employed to screen small molecules from MCULE's library of investigational chemical compounds are shown in Table 4.1. 2 ligand molecules best fitted into the binding pocket of HER2 and satisfied the applied druglikeness criteria of RO5, PSA, MR, RBs, N and O atoms, and NRs as discussed in methodology depicted as an outcome of SBVS. SBVS-hits were subsequently subjected to MCULE toxicity check, SwissADME filters, multi-scoring docking via ADV, ΔG comparable to known inhibitors of target protein viz., Lapatinib, Neratinib, and Tucatinib, and MD simulation of 10 ns duration.

Table 4.1: Top 100 ligand hits obtained after SBVS

S. No.	**Ligands**	**Binding energy (kcal/mol)**	**RO5 violations**
1	MCULE-9386350598	-10.1	0
2	MCULE-9083675198	-9.9	0
3	MCULE-8937595731	-9.9	0
4	MCULE-2082061687	-9.8	0
5	MCULE-9841320064	-9.7	0
6	MCULE-9514587152	-9.7	0
7	MCULE-9081505108	-9.6	0
8	MCULE-8016227151	-9.5	0
9	MCULE-7438970158	-9.5	0
10	MCULE-7732897976	-9.5	0
11	MCULE-1217969814	-9.4	0
12	MCULE-6732922117	-9.4	0
13	MCULE-9503708560	-9.3	0
14	MCULE-7599568441	-9.2	0
15	MCULE-3773590316	-9.2	0
16	MCULE-4420319124	-9.1	0
17	MCULE-3261949500	-9.1	0

18	MCULE-7002197612	-9	0
19	MCULE-6455149784	-8.9	0
20	MCULE-3840783663	-8.9	0
21	MCULE-4544985274	-8.9	0
22	MCULE-1196681046	-8.9	0
23	MCULE-9433162170	-8.8	0
2	MCULE-8028742001	-8.8	0
25	MCULE-4924578810	-8.8	0
26	MCULE-4638340739	-8.8	0
27	MCULE-2116801361	-8.8	0
28	MCULE-5671860004	-8.7	0
29	MCULE-1800565896	-8.7	0
30	MCULE-6264951729	-8.7	0
31	MCULE-5984253496	-8.6	0
32	MCULE-8109420073	-8.6	0
33	MCULE-7057324381	-8.6	0
34	MCULE-8782640423	-8.6	0
35	MCULE-1558627453	-8.5	0
36	MCULE-7224872978	-8.5	0
37	MCULE-2454948452	-8.5	0
38	MCULE-9629714723	-8.5	0
39	MCULE-7225215567	-8.5	0
40	MCULE-7093625408	-8.4	0
41	MCULE-6232409085	-8.4	0
42	MCULE-8046841408	-8.4	0
43	MCULE-6524304771	-8.4	0
44	MCULE-9038810560	-8.3	0
45	MCULE-8379109255	-8.3	0
46	MCULE-2132659354	-8.3	0
47	MCULE-5039509090	-8.3	0

48	MCULE-4577280534	-8.3	0
49	MCULE-7256289530	-8.3	0
50	MCULE-4042431771	-8.3	0
51	MCULE-8752115040	-8.3	0
52	MCULE-5180351602	-8.2	0
53	MCULE-1328505063	-8.2	0
54	MCULE-7045636868	-8.2	0
55	MCULE-5613555964	-8.2	0
56	MCULE-7443327368	-8.2	0
57	MCULE-1355912164	-8.2	0
58	MCULE-2860715238	-8.2	0
59	MCULE-6864921967	-8.1	0
60	MCULE-1986483046	-8.1	0
61	MCULE-3712977841	-8.1	0
62	MCULE-8134998711	-8.1	0
63	MCULE-6081257779	-8.1	0
64	MCULE-7564250835	-8.1	0
65	MCULE-8371770867	-8.1	0
66	MCULE-6661875109	-8	0
67	MCULE-1273749701	-8	0
68	MCULE-4616972123	-8	0
69	MCULE-8682692956	-8	0
70	MCULE-1200107886	-8	0
71	MCULE-4297750503	-8	0
72	MCULE-4862665716	-8	0
73	MCULE-1028628572	-8	0
74	MCULE-8084678579	-8	0
75	MCULE-9435046411	-8	0
76	MCULE-3963628408	-8	0
77	MCULE-4366901925	-8	0

78	MCULE-3803731002	-7.9	0
79	MCULE-1633822804	-7.9	0
80	MCULE-2830496140	-7.9	0
81	MCULE-7354085546	-7.9	0
82	MCULE-7721983483	-7.9	0
83	MCULE-5302780192	-7.9	0
84	MCULE-1120416301	-7.9	0
85	MCULE-9019088305	-7.9	0
86	MCULE-5422302495	-7.8	0
87	MCULE-6096281367	-7.8	0
88	MCULE-8091079105	-7.8	0
89	MCULE-6565724311	-7.8	0
90	MCULE-2577974654	-7.8	0
91	MCULE-4063820706	-7.8	0
92	MCULE-8765619407	-7.8	0
93	MCULE-1726158340	-7.8	0
94	MCULE-9917566553	-7.8	0
95	MCULE-2621480900	-7.8	0
96	MCULE-2655859613	-7.8	0
97	MCULE-5279356278	-7.8	0
98	MCULE-7280319389	-7.8	0
99	MCULE-8398142176	-7.8	0
100	MCULE-8967790570	-7.8	0

Toxicity risk assessment

Molecular toxicity and poor pharmacokinetics of clinical drug candidates is significant issue for costly late-stage attrition in the biological evaluation of the drug development process. In the early stages of small-molecule drug discovery campaigns, it is highly desirable to filter out such compounds that contain carcinogenic and mutagenic moieties, scaffolds, and toxicophores. During MCULE's toxicity risk assessment, only 49 compounds came out as successful drug candidates, and the remaining 61 ligands were rejected are shown in Table

4.2. MCULE toxicity checker precludes potentially toxic compounds from hit identification list using robust SMARTS algorithm that works through investigating specific chemical patterns in an existing virtual library of small molecules and thus save both cost and valuable time spending on undesired chemical molecules (Kiss R et al., 2008, Shakil S et al., 2019, Wu J et al., 2013, Watts C. A et al., 2013, Zhang W et al., 2016, Daina A et al., 2017, OLEG TROTT A. J. O et al., 2010, Ajijur R et al., 2021, Khan M. K. A., 2018, Ahmad K. M. K 2020, Khan M. K. A et al., 2018, Khan M. K. A et al., 2020, Zoete V., 2010, Van Der Spoel D., 2005, Vanommeslaeghe K., 2012, Vanommeslaeghe K et al., 2010, Petersen H. G et al., 1995, Stenberg S et al., 2020, Fischer N. M et al., 2015).

Table 4.2: Ligand hits succeeded toxicity check

S. No.	**Ligands**	**Toxicity Pass**
1	MCULE-9386350598	Passed
2	MCULE-9083675198	Passed
3	MCULE-2082061687	Passed
4	MCULE-9514587152	Passed
5	MCULE-8016227151	Passed
6	MCULE-4420319124	Passed
7	MCULE-7002197612	Passed
8	MCULE-3840783663	Passed
9	MCULE-4544985274	Passed
10	MCULE-9433162170	Passed
11	MCULE-8028742001	Passed
12	MCULE-4638340739	Passed
13	MCULE-2116801361	Passed
14	MCULE-5671860004	Passed
15	MCULE-6264951729	Passed
16	MCULE-5984253496	Passed
17	MCULE-8109420073	Passed
18	MCULE-7057324381	Passed

19	MCULE-8782640423	Passed
20	MCULE-1558627453	Passed
21	MCULE-2454948452	Passed
22	MCULE-7093625408	Passed
23	MCULE-6232409085	Passed
24	MCULE-8046841408	Passed
25	MCULE-9038810560	Passed
26	MCULE-2132659354	Passed
27	MCULE-7256289530	Passed
28	MCULE-4042431771	Passed
29	MCULE-8752115040	Passed
30	MCULE-5180351602	Passed
31	MCULE-1328505063	Passed
32	MCULE-7045636868	Passed
33	MCULE-5613555964	Passed
34	MCULE-7443327368	Passed
35	MCULE-1355912164	Passed
36	MCULE-2860715238	Passed
37	MCULE-1986483046	Passed
38	MCULE-6081257779	Passed
39	MCULE-4616972123	Passed
40	MCULE-4297750503	Passed
41	MCULE-4862665716	Passed
42	MCULE-1028628572	Passed
43	MCULE-8084678579	Passed
44	MCULE-1633822804	Passed
45	MCULE-5302780192	Passed
46	MCULE-4063820706	Passed
47	MCULE-1726158340	Passed
48	MCULE-9917566553	Passed

49	MCULE-7280319389	Passed

Absorption, distribution, metabolism, and excretion prediction

Brain Or IntestinaL EstimateD (BOILED)-Egg permeation predictive model of SwissADME tool was used to screen the toxicity-filtered small molecules. The BOILED-Egg model, a.k.a. Egan Egg that predicts a threshold for two key ADME parameters concurrently viz., the passive gastrointestinal absorption (HIA) and blood-brain barrier (BBB) access (WLOGP ≤ 5.88 and TPSA ≤ 131.6, for lipophilicity and apparent polarity) and a clear schematic illustration of how far a compound is from the perfect one for ideal absorption (Hevener K. E et., 2018, Attique S et al., 2019, Egan W.J et al., 2000) As the name sounds, the model consists of the yolk (yellow) and white regions that depict the physicochemical locations for most plausible BBB permeation and most promising gastrointestinal tract absorption, respectively. All toxicity-successful chemical hits were found within BBB permeation and HIA absorption physiochemical spaces and were comparatively better than selected inhibitors. Chemical molecules located within the yolk (yellow) region depicted a high propensity for BBB permeation, and ligands occupied by the white region exhibited a greater tendency towards HIA. The blue and red dots represent P-gp positive and P-gp negative molecules, respectively (Figure 4.1). Inhibitor Lapatinib and Neratinib is located outside the Egg, meaning negligible absorption, but it shows BBB permeation although P-gp effluxes it. Inhibitor Tucatinib showed plausible absorption but negligible brain penetration. Fifteen chemical hits were found P-gp positive, and the remaining 45 molecules succeeded the BOILED-Egg criterion of ADME filtration. Ligand hits (blue dots) thrown out from the brain were rejected and not brought forward for molecular interaction study (Figure 4.1).

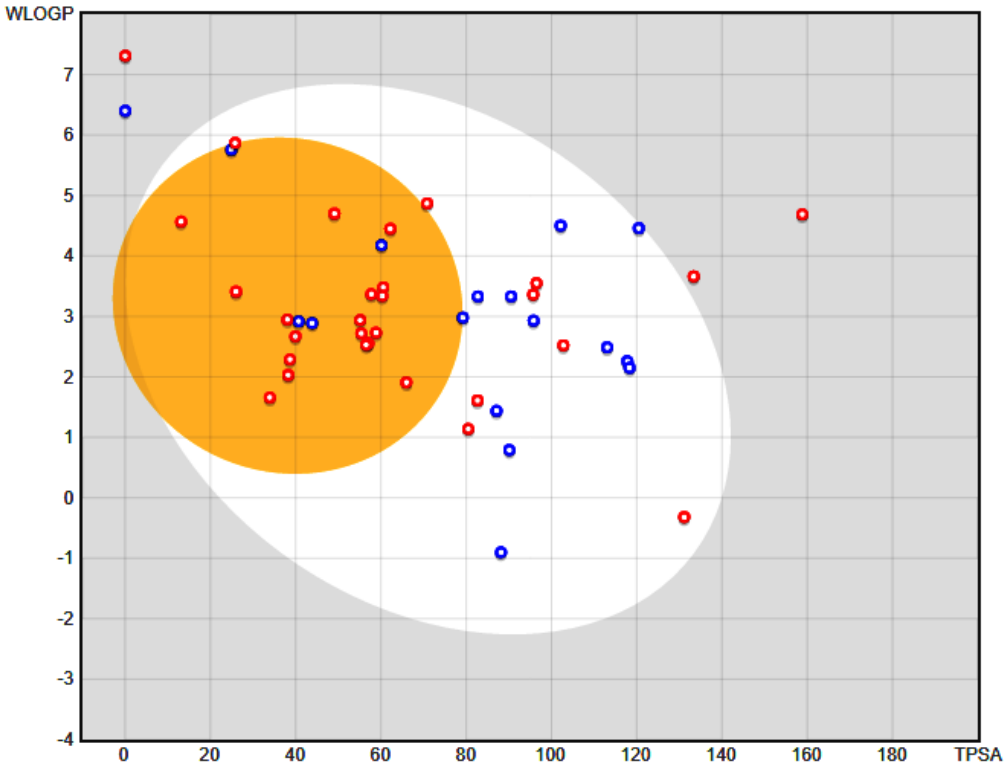

Figure 4.1: Evaluation of passive gastrointestinal absorption (HIA) and blood-brain barrier (BBB) access in the function of the position of ligand hits and selected inhibitors using the BOILED-Egg model.

Physicochemical properties

Molecular weight (MW), the fraction of carbons in the sp3 hybridization (FCsp3), rotatable bond (RB), hydrogen bond acceptor (HBA), hydrogen bond donor (HBD), molar refractivity (MR), and polar surface area (PSA), key molecular and physicochemical descriptors play an essential role in the quick prediction of ADME attributes of investigational ligand molecules. SwissADME relies on OpenBabel v2.3.0 to compute the ADME features mentioned above features. Moreover, SwissADME uses a fragmental technique to estimate the PSA of chemical compounds, usually known as topological polar surface area (TPSA) (Egan W. J et al., 2002, O'Boyle N. M et al., 2002). All ligand hits (45) that succeeded the BOILED-Egg model was found in the acceptable range of aforesaid physicochemical properties except the FCsp3. 25 out of 39 ligand hits showed the FCsp3 value less than 0.25. Known inhibitors of HER2 viz., Lapatinib, Neratinib and Tucatinib respectively exhibited three (MW: 581.06 g/m; RB: 11; MR: 153.88), two (MW: 557.04; $FCsp^3$: 0.2), and one ($FCsp^3$: 0.17) violations

of physicochemical properties (Ertl Pet al., 2000, Veber D.F et al., 2002). Details of physicochemical properties of the BOILED-Egg passed small molecules and inhibitors are shown in Table 4.3.

Table 4.3: Physicochemical properties of small molecules (BOILED-Egg filtered ligand hits) and known inhibitors.

S. No.	**Ligands**	**MW (g/mol)**	**FCsp3**	**RB**	**HBA**	**HBD**	**MR**	**TPSA (Å²)**
1.	MCULE-9083675198	334.42	0.06	0	4	0	92.29	102.16
2.	MCULE-2082061687	321.72	0.23	4	7	1	77.76	113.09
3.	MCULE-9514587152	282.36	0.27	4	3	1	79.41	82.7
4.	MCULE-8016227151	317.31	0	3	5	0	78.27	70.81
5.	MCULE-4420319124	312.12	0.08	3	4	1	66.48	24.92
6.	MCULE-7002197612	312.15	0.31	3	5	0	75.81	60.51
7.	MCULE-3840783663	263.4	0.6	2	2	0	80.59	40.71
8.	MCULE-4544985274	257.33	0.13	3	2	0	73.08	49.09
9.	MCULE-9433162170	236.23	0	1	4	0	66.43	56.74
10.	MCULE-8028742001	268.1	0.1	1	3	1	65.55	58.87
11.	MCULE-4638340739	241.29	0.47	2	3	0	72.04	38.66
12.	MCULE-	227.69	0	0	0	1	68.28	26.02

	5671860004							
13.	MCULE-5984253496	334.09	0.33	4	12	0	42.72	9.23
14.	MCULE-8109420073	304.14	0.08	3	3	0	72.16	39.94
15.	MCULE-7057324381	335.35	0.54	4	5	2	83.09	90.5
16.	MCULE-8782640423	400.58	0.67	6	13	1	54.44	37.91
17.	MCULE-1558627453	246.31	0.46	4	3	1	75.06	57.06
18.	MCULE-2454948452	256.35	0.47	4	3	0	79.31	33.95
19.	MCULE-7093625408	306.28	0.25	6	6	3	76.02	131.14
20.	MCULE-6232409085	238.25	0.17	1	4	1	65.22	82.66
21.	MCULE-8046841408	250.71	0	1	2	2	66.62	95.83
22.	MCULE-9038810560	248.24	0.45	3	6	1	62.11	90.14
23.	MCULE-2132659354	345.93	0.11	1	5	0	62.26	25.78
24.	MCULE-7256289530	295.18	0.31	3	2	1	71.85	38.05
25.	MCULE-4042431771	302.35	0.2	6	4	1	79.18	96.51
26.	MCULE-8752115040	253.3	0.2	2	3	0	75.15	38.25
27.	MCULE-	292.4	0.46	7	3	3	83.48	117.81

	5180351602							
28.	MCULE-1328505063	304.15	0.08	2	3	1	72.99	55.11
29.	MCULE-7045636868	310.44	0.06	2	1	0	103.09	60.11
30.	MCULE-5613555964	343.42	0.29	3	3	0	105.13	57.74
31.	MCULE-7443327368	216.24	0.17	3	3	2	60.26	65.98
32.	MCULE-1355912164	261.34	0.21	4	2	0	74.66	56.53
33.	MCULE-2860715238	328.25	0.33	5	10	1	71.06	102.78
34.	MCULE-6081257779	279.34	0.62	6	5	3	78.8	88.17
35.	MCULE-4616972123	383.4	0.25	10	7	1	102.66	95.71
36.	MCULE-4297750503	372.44	0.47	5	8	0	100.64	118.3
37.	MCULE-4862665716	231.29	0.54	3	3	0	65.08	43.85
38.	MCULE-1028628572	325.86	0.08	4	3	0	82.23	120.45
39.	MCULE-8084678579	272.32	0.07	3	3	0	74.45	60.34
40.	MCULE-1633822804	285.36	0.2	6	4	1	79.48	79.19
41.	MCULE-5302780192	204.31	0.57	1	1	0	65.04	13.14
42.	MCULE-	278.38	0.58	6	3	1	76.84	87.11

	4063820706							
43.	MCULE-1726158340	335.22	0.07	3	1	1	82.83	62.19
44.	MCULE-9917566553	207.25	0.1	1	3	0	54.84	55.41
45.	MCULE-7280319389	227.63	0.12	2	5	2	51.31	80.48
46.	Tucatinib-inhibitor	480.52	0.19	6	7	2	141.66	110.85
47.	Lapatinib-inhibitor	581.06	0.17	11	8	2	153.88	114.73
48.	Neratinib-inhibitor	557.04	0.2	12	7	2	157.05	112.4

Reference range: MW ≤ 500 g/m, HBA ≤ 10, HBD ≤ 5 (Lipinski et al., 2012) (50), $FCsp^3$ ≥ 0.25 (Daina et al., 2017), RB ≤ 10 (Veber et al., 2002), 40 ≤ MR ≤ 130 (Ghose et al., 1999), TPSA≤ 150 (Muegge et al., 2001)

Lipophilicity

Lipophilicity is a molecule's most important physical property: its solubility absorption, plasma protein binding, metabolic clearance, the volume of distribution, enzyme and receptor binding, biliary and renal clearance, brain penetration, and storage in tissues bioavailability, and toxicity. It can be defined as a partition coefficient between n-octanol and water (Log Po/w). Mathematically, it can be expressed as-.

Log Po/w = log $[\text{ligand molecule}]_{\text{octanol}}$ / $[\text{ligand molecule}]_{\text{water}}$

Lipophilicity of all selected molecules were evaluated using three different descriptors of SwissADME viz., Log Po/w (XLogP3) (Ghose A. K et al., 1999, Muegge I et al., 2001) Log Po/w (WLogP) (Ghose A. K et al., 1999), and Log Po/w (MLogP) (Ghose A. K et al., 1999, Ertl P et al., 2000). All chemical hits were bound lipophilic as their Log Po/w values exhibited in the specified range of XLogP3 (-2 to 5), WLogP (-0.4 to 5.88), and MLogP (≤ 4.15). As compared to known inhibitors, selected ligands exhibited better lipophilicity. Lapatinib and Neratinib showed slightly greater values than the optimum value of XLogP3.

Values of WLogP and MLogP of both were found in the optimum range. In comparison, inhibitor Tucatinib portrayed all LogP values in the acceptable range. Details of computed lipophilicity of ligand molecules and inhibitors are shown in Table 4.4.

Table 4.4: Computed lipophilicity of small molecules (BOILED-Egg filtered ligand hits) and known inhibitors.

S. No.	**Ligands**	**Log $P_{o/w}$ (XLogP3)**	**Log $P_{o/w}$ (WLogP)**	**Log $P_{o/w}$ (MLogP)**
1.	MCULE-9083675198	4.85	4.5	2.8
2.	MCULE-2082061687	2.21	2.49	1.63
3.	MCULE-9514587152	3.25	3.33	1.87
4.	MCULE-8016227151	4.39	4.87	3.16
5.	MCULE-4420319124	4	5.76	3.35
6.	MCULE-7002197612	3.55	3.48	2.65
7.	MCULE-3840783663	2.24	2.92	2.49
8.	MCULE-4544985274	3.81	4.7	4.18
9.	MCULE-9433162170	3.52	2.56	1.72
10.	MCULE-8028742001	3.2	2.73	2.99
11.	MCULE-4638340739	2.76	2.29	2.29
12.	MCULE-5671860004	3.89	3.41	4.05
13.	MCULE-5984253496	4.69	8.88	5.34
14.	MCULE-8109420073	3.7	2.67	3.77
15.	MCULE-7057324381	1.25	3.33	2.24
16.	MCULE-8782640423	4.89	9.38	3.18
17.	MCULE-1558627453	2.45	2.56	1.03
18.	MCULE-2454948452	2.77	1.66	2.62
19.	MCULE-7093625408	-1.02	-0.32	-1.67
20.	MCULE-6232409085	0.76	1.61	0.48

21.	MCULE-8046841408	2.61	2.93	1.91
22.	MCULE-9038810560	-0.19	0.79	-0.54
23.	MCULE-2132659354	4.71	5.87	4.08
24.	MCULE-7256289530	2.78	2.95	2.66
25.	MCULE-4042431771	2.88	3.55	1.01
26.	MCULE-8752115040	2.27	2.03	1.41
27.	MCULE-5180351602	2.49	2.26	0.85
28.	MCULE-1328505063	2.52	2.94	2.14
29.	MCULE-7045636868	4.86	4.18	3.62
30.	MCULE-5613555964	5.02	3.37	2.61
31.	MCULE-7443327368	2.55	1.91	0.79
32.	MCULE-1355912164	1.92	2.53	2.41
33.	MCULE-2860715238	1.45	2.52	0.36
34.	MCULE-6081257779	-0.7	-0.9	-1.17
35.	MCULE-4616972123	3.85	3.36	1.61
36.	MCULE-4297750503	1.68	2.15	0.36
37.	MCULE-4862665716	2.15	2.89	1.33
38.	MCULE-1028628572	3.95	4.46	1.66
39.	MCULE-8084678579	2.6	3.34	2.82
40.	MCULE-1633822804	2.04	2.98	0.39
41.	MCULE-5302780192	3.9	4.57	3.16
42.	MCULE-4063820706	2.07	1.44	0.35
43.	MCULE-1726158340	4.39	4.45	2.77
44.	MCULE-9917566553	1.79	2.72	1.26
45.	MCULE-7280319389	0.86	1.14	1.62
46.	Tucatinib- inhibitor	3.99	4.52	3.01
47.	Lapatinib- inhibitor	5.12	7.34	3.44

48.	Neratinib- inhibitor	4.87	5.59	1.64

Reference range: XLogP3 (-2 to 5) (53,54); WLogP (-0.4 to 5.88) (53,46,47); MLogP (≤ 4.15).

Solubility

Solubility is the maximum dissolved concentration in a solvent at given conditions. It determines intestinal absorption and oral bioavailability. Low solubility limits absorption and causes low oral bioavailability. Molecular properties for solubility and permeability are opposed. Good solubility is essential for intravenous formulation. SwissADME uses three descriptors adapted from the ESOL model, Ali et al., 2012, and SILICOS-IT filter to predict the water solubility of small molecules at log S scale, which is a decimal logarithm of the molar solubility in water. Optimum range for water solubility follows the order as insoluble <−10 < poorly <−6 < moderately <−4 < soluble <−2 < very < 0 < highly. Computed water solubilities of ligands and inhibitors revealed that they fall either in the soluble, moderate soluble or poorly soluble category (Table 4.5).

Table 4.5: Computed solubility of small molecules (BOILED-Egg filtered ligand hits) and known inhibitors.

S. No.	**Ligands**	**Log *S* (ESOL)**	**Log *S* (Ali)**	**Log *S* (SILICOS-IT)**
1.	MCULE-9083675198	-5.61	-6.73	-7.35
2.	MCULE-2082061687	-3.5	-4.22	-5.17
3.	MCULE-9514587152	-3.97	-4.66	-5.79
4.	MCULE-8016227151	-4.95	-5.59	-6.87
5.	MCULE-4420319124	-4.62	-4.23	-6.31
6.	MCULE-7002197612	-4.22	-4.51	-5.89
7.	MCULE-3840783663	-2.96	-2.73	-3.77
8.	MCULE-4544985274	-4.13	-4.54	-6.19
9.	MCULE-9433162170	-4.2	-4.4	-4.75
10.	MCULE-8028742001	-4.06	-4.11	-4.69

11.	MCULE-4638340739	-3.19	-3.23	-3.42
12.	MCULE-5671860004	-4.26	-4.13	-5.26
13.	MCULE-5984253496	-4.81	-4.61	-5.33
14.	MCULE-8109420073	-4.48	-4.23	-5.21
15.	MCULE-7057324381	-2.64	-2.75	-3.78
16.	MCULE-8782640423	-5.16	-5.42	-5.22
17.	MCULE-1558627453	-2.89	-3.29	-3.61
18.	MCULE-2454948452	-3.34	-3.14	-3.86
19.	MCULE-7093625408	-1.04	-1.25	-1.46
20.	MCULE-6232409085	-2.31	-2.08	-3.94
21.	MCULE-8046841408	-3.62	-4.27	-4.59
22.	MCULE-9038810560	-1.43	-1.25	-3.07
23.	MCULE-2132659354	-5.32	-4.98	-6.26
24.	MCULE-7256289530	-3.7	-3.24	-4.42
25.	MCULE-4042431771	-3.66	-4.57	-5.58
26.	MCULE-8752115040	-3.18	-2.71	-4.5
27.	MCULE-5180351602	-3.17	-4.61	-5.2
28.	MCULE-1328505063	-3.8	-3.32	-5.14
29.	MCULE-7045636868	-5.12	-5.86	-5.72
30.	MCULE-5613555964	-5.42	-5.97	-6.11
31.	MCULE-7443327368	-3.1	-3.58	-3.92
32.	MCULE-1355912164	-2.9	-2.73	-4.66
33.	MCULE-2860715238	-2.84	-3.21	-4.82
34.	MCULE-6081257779	-0.96	-0.68	-3.96
35.	MCULE-4616972123	-4.43	-5.56	-7.05
36.	MCULE-4297750503	-3.33	-3.78	-5.41
37.	MCULE-4862665716	-2.87	-2.7	-3.73

38.	MCULE-1028628572	-4.71	-6.18	-5.96
39.	MCULE-8084678579	-3.55	-3.52	-4.93
40.	MCULE-1633822804	-3.09	-3.33	-6.43
41.	MCULE-5302780192	-3.74	-3.87	-4.79
42.	MCULE-4063820706	-2.86	-3.53	-3.24
43.	MCULE-1726158340	-5.07	-5.41	-6
44.	MCULE-9917566553	-2.72	-2.57	-4.02
45.	MCULE-7280319389	-2.2	-2.13	-3.6
46.	Tucatinib- inhibitor	-5.45	-6.02	-9.12
47.	Lapatinib- inhibitor	-6.44	-7.27	-12.49
48.	Neratinib- inhibitor	-5.98	-6.97	-10.15

Reference values: insoluble <−10 < poorly <−6 < moderately <−4 < soluble <−2 < very < 0 < highly.

Pharmacokinetics

Pharmacokinetics (PK) plays a crucial role in determining the safety and efficacy of a therapeutic molecule. PK describes the response of the biological system when drug molecules pass through it in terms of ADME. The absorption (A), distribution (D) features of selected ligands and inhibitors have been discussed in the previous section of the BOILED-Egg model of ADME. Biotransformation of therapeutic molecules through phase I metabolizing enzymes, especially cytochrome P450 isozymes (CYP450s), is an essential aspect of their metabolism (M) and excretion (E). SwissADME predicts whether a drug molecule is a substrate or inhibitor of five major CYP450s viz., CYP1A2, CYP2C19, CYP2C9, CYP2D6, and CYP3A4. Inhibiting these CYP450 isozymes causes toxicity and undesirable effects due to the lower excretion and accrual of ingested drug molecules. The propensity of ligand hits towards the skin permeation (log Kp) were predicted and found comparable to the selected inhibitors. The more negative the log Kp value lower the skin permeation (Potts R. O et al., 1992).The details of predicted CYP450s metabolism and skin permeation of ligands and inhibitors are shown in Table 4.6.

Table 4.6: Computed pharmacokinetic features of small molecules (BOILED-Egg filtered ligand hits) and known inhibitors.

S. No.	**Ligands**	**CYP1A2**	**CYP2C19**	**CYP2C9**	**CYP2D6**	**CYP3A4**	**Log K_p (cm/s)**
		Inhibitor					
1.	MCULE-9083675198	Yes	No	Yes	No	Yes	-4.9
2.	MCULE-2082061687	Yes	No	No	No	No	-6.69
3.	MCULE-9514587152	Yes	Yes	Yes	Yes	Yes	-5.71
4.	MCULE-8016227151	Yes	Yes	Yes	No	No	-5.12
5.	MCULE-4420319124	Yes	Yes	No	Yes	No	-5.39
6.	MCULE-7002197612	Yes	Yes	Yes	No	No	-5.68
7.	MCULE-3840783663	No	No	Yes	Yes	No	-6.32
8.	MCULE-4544985274	Yes	Yes	No	No	No	-5.16
9.	MCULE-9433162170	Yes	Yes	No	No	No	-5.24
10.	MCULE-8028742001	Yes	Yes	No	No	No	-5.66
11.	MCULE-4638340739	No	Yes	No	Yes	No	-5.81
12.	MCULE-5671860004	Yes	Yes	Yes	No	No	-4.93

13.	MCULE-5984253496	No	No	No	No	No	-5.01
14.	MCULE-8109420073	Yes	Yes	Yes	No	No	-5.53
15.	MCULE-7057324381	No	No	No	No	No	-7.46
16.	MCULE-8782640423	No	Yes	Yes	No	No	-5.27
17.	MCULE-1558627453	Yes	Yes	No	No	No	-6.06
18.	MCULE-2454948452	No	No	No	No	No	-5.9
19.	MCULE-7093625408	No	No	No	No	No	-8.89
20.	MCULE-6232409085	Yes	No	No	No	No	-7.21
21.	MCULE-8046841408	Yes	Yes	No	No	No	-5.98
22.	MCULE-9038810560	Yes	No	No	No	No	-7.95
23.	MCULE-2132659354	No	No	Yes	No	No	-5.07
24.	MCULE-7256289530	Yes	Yes	No	Yes	No	-6.13
25.	MCULE-4042431771	Yes	Yes	Yes	Yes	Yes	-6.1
26.	MCULE-8752115040	Yes	No	No	No	No	-6.23
27.	MCULE-5180351602	Yes	No	No	No	Yes	-6.32

28.	MCULE-1328505063	Yes	Yes	No	Yes	Yes	-6.37
29.	MCULE-7045636868	Yes	No	Yes	No	No	-4.74
30.	MCULE-5613555964	Yes	Yes	Yes	No	Yes	-4.83
31.	MCULE-7443327368	Yes	No	No	No	No	-5.81
32.	MCULE-1355912164	Yes	Yes	No	No	No	-6.53
33.	MCULE-2860715238	Yes	No	No	No	Yes	-7.27
34.	MCULE-6081257779	No	No	No	No	No	-8.5
35.	MCULE-4616972123	Yes	Yes	Yes	Yes	Yes	-5.91
36.	MCULE-4297750503	No	No	Yes	No	Yes	-7.38
37.	MCULE-4862665716	Yes	Yes	No	No	No	-6.18
38.	MCULE-1028628572	Yes	Yes	Yes	No	Yes	-5.48
39.	MCULE-8084678579	Yes	Yes	No	No	No	-6.12
40.	MCULE-1633822804	Yes	Yes	Yes	Yes	Yes	-6.59
41.	MCULE-5302780192	No	No	No	Yes	No	-4.78
42.	MCULE-4063820706	No	No	No	No	No	-6.53

43.	MCULE-1726158340	Yes	Yes	Yes	No	Yes	-5.23
44.	MCULE-9917566553	Yes	No	No	No	No	-6.29
45.	MCULE-7280319389	No	No	No	No	No	-7.08
46.	Tucatinib-inhibitor	Yes	Yes	Yes	Yes	Yes	-6.4
47.	Lapatinib-inhibitor	No	Yes	Yes	Yes	Yes	-6.21
48.	Neratinib-inhibitor	No	Yes	Yes	Yes	Yes	-6.24

Druglikeness and Medicinal chemistry attributes

SwissADME tool uses five different pharmaceutical and biotechnology-based rules with diverse arrays of filters that qualitatively forecast the propensity for a molecule to become a putative oral drug candidate concerning bioavailability. The BOILED-Egg sifted all ligand hits (39 molecules) showed no violations of Pfizer's RO5. Single ligand (out of 39) showed one violation (WLogP > 5.6) of Amgen's Ghose filters (160 ≤ MW ≤ 480, -0.4 ≤ WLogP ≤ 5.6, 40 ≤ MR ≤ 130, 20 ≤ Atoms ≤ 70) (Martin Y. C.,2005). Two ligands (out of 39) exhibited one violation (XLogP3 > 5) of Bayer's Muegge filters (200 ≤ MW ≤ 600, -2 ≤ XLogP3 ≤ 5, TPSA ≤ 150, No. of C > 4, No. of heteroatoms > 1, RB ≤ 15, HBA ≤ 10, HBD ≤ 5) (Baell J. B et al., 2010). No ligand hits displayed any single violation of Pharmacia's Egan parameters (WLogP ≤ 5.88, TPSA ≤ 131.6) and GlaxoSmithKline's Veber filters (RB ≤ 10, TPSA ≤ 140) [46,51].Inhibitor AZ82 exhibited one violation of each RO5 (MW > 500), Veber (RB > 10), Muegge filters (XLogP3 > 5), and three violations of Ghose filters (MW > 480, WLogP > 5.6, MR > 130). Inhibitor CW069 displayed one violation of each RO5 (MW > 500) and Ghose filters (MW > 480). Inhibitor SR31527 showed a single violation of Muegge filters (XLogP3 > 5).

Abbott bioavailability score (BS) is a determinant of the oral absorption of a drug molecule. Although, similar physical properties do not apply to cations, anions, and uncharged

molecules at physiologic pH, delineating their bioavailability and permeability. PSA for anions and RO5 for both cations and uncharged molecules have pretty enough forecasting ability. Abbot BS is 0.11 for anions showing PSA >150 Å2, 0.56 if PSA ranging 75-150 Å2, and 0.85 if PSA is less than 75 Å2. Abbot BS is 0.55 and 0.17 respectively for remaining compounds that comply and breach RO5 (Martin Y. C et al., 2005). All virtually screened ligands and reference inhibitors exhibit an Abbott BS value of 0.55 means they fulfilled the criteria of oral drug molecules.

In medicinal chemistry attributes evaluation, respectively, one and eight ligands were depicted as frequent hitters, i.e., Pan Assay Interference Structure (PAINS) alert and undesirable compounds, i.e., Brenk alert (Brenk R et al., 2008). Moreover, seventeen and six ligand hits displayed 1 and 2 leadlikeness (LL) ($250 \leq MW \leq 350$, $XLogP \leq 3.5$, $RB \leq 7$) violations (Teague S. J et al., 1999). Synthetic accessibility (SA) is an essential determinant of chemical synthesis for virtual molecules. Respectively 1 and 10 SA value represents very easy and very difficult synthesis modes (Ertl P et al., 2009). All molecules, including reference inhibitors, depicted an accessible mode of their synthesis ($SA < 5$). Respectively 3 ($MW > 350$, $RB > 7$, $XLogP3 > 3.5$), 2 ($MW > 350$, $RB > 7$) and 1 ($XLogP3 > 3.5$) LL violations by AZ82, CW069, and SR31527 and I Brenk alert by each CW069, and SR31527 were observed in the medicinal chemistry attribute assessment. Details of computed druglikeness and medicinal chemistry of ligands and inhibitors are shown in Table 4.7.

Table 4.7: Computed druglikeness and medicinal chemistry attributes of small molecules (BOILED-Egg filtered ligand hits) and known inhibitors.

S. No.	**Ligands**	**Druglikeness**						**Medicinal chemistry attributes**			
		RO 5	**Ghose**	**Veber**	**Egan**	**Muegge**	***BS**	**PS ^**	**BK &**	**#LL violation(s)**	**$SA**
		violation(s)						**alert(s)**			
1.	MCULE-908367519 8	No	No	No	No	No	0.55	0	0	1	3.05
2.	MCULE-	No	No	No	No	No	0.5	0	0	No	3.8

	2082061687						5				7
3.	MCULE-9514587152	No	No	No	No	No	0.55	0	0	No	3.02
4.	MCULE-8016227151	No	No	No	No	No	0.55	0	0	1	3.11
5.	MCULE-4420319124	No	1	No	No	No	0.55	0	0	1	2.12
6.	MCULE-7002197612	No	No	No	No	No	0.55	0	2	1	3.5
7.	MCULE-3840783663	No	No	No	No	No	0.55	0	1	No	3.88
8.	MCULE-4544985274	1	No	No	No	No	0.55	0	0	1	2.31
9.	MCULE-9433162170	No	No	No	No	No	0.55	0	0	2	2.7
10.	MCULE-8028742001	No	No	No	No	No	0.55	0	0	No	2.5
11.	MCULE-4638340739	No	No	No	No	No	0.55	0	0	1	3.99
12.	MCULE-56718600	No	No	No	No	1	0.55	0	2	2	2.27

	04										
13.	MCULE-5984253496	No	No	No	1	2	0.55	0	2	1	2.79
14.	MCULE-8109420073	No	No	No	No	No	0.55	0	0	1	2.84
15.	MCULE-7057324381	No	No	No	No	No	0.55	0	0	No	3.4
16.	MCULE-8782640423	No	1	No	1	1	0.55	0	1	2	3.38
17.	MCULE-1558627453	No	No	No	No	No	0.55	1	1	1	2.89
18.	MCULE-2454948452	No	No	No	No	No	0.55	0	0	No	2.64
19.	MCULE-7093625408	No	No	No	No	No	0.56	0	0	No	2.83
20.	MCULE-6232409085	No	No	No	No	No	0.55	0	0	1	2.45
21.	MCULE-8046841408	No	No	No	No	No	0.55	1	0	No	2.51
22.	MCULE-90388105	No	No	No	No	No	0.55	0	0	1	2.96

	60										
23.	MCULE-2132659354	No	No	No	No	No	0.55	0	0	1	1.99
24.	MCULE-7256289530	No	No	No	No	No	0.55	0	0	No	2.17
25.	MCULE-4042431771	No	No	No	No	No	0.55	0	0	No	3.62
26.	MCULE-8752115040	No	No	No	No	No	0.55	0	1	No	2.87
27.	MCULE-5180351602	No	No	No	No	No	0.55	0	0	No	2.91
28.	MCULE-1328505063	No	NO	No	No	No	0.55	0	0	No	2.91
29.	MCULE-7045636868	No	No	No	No	No	0.55	1	2	1	4.46
30.	MCULE-5613555964	No	No	No	No	1	0.55	0	0	1	3.63
31.	MCULE-7443327368	No	No	No	No	No	0.55	0	0	1	1.97
32.	MCULE-13559121	No	No	No	No	No	0.55	0	0	0	2.52

	64										
33.	MCULE-2860715238	No	No	No	No	No	0.55	0	0	0	2.69
34.	MCULE-6081257779	No	1	No	No	No	0.55	0	0	0	3.33
35.	MCULE-4616972123	No	No	No	No	No	0.55	0	0	3	3.37
36.	MCULE-4297750503	No	No	No	No	No	0.55	0	0	1	4.38
37.	MCULE-4862665716	No	No	No	No	No	0.55	0	0	1	2.87
38.	MCULE-1028628572	No	No	No	No	No	0.55	0	0	1	3.05
39.	MCULE-8084678579	No	No	No	No	No	0.55	0	0	No	2.91
40.	MCULE-1633822804	No	No	No	No	No	0.55	0	0	No	3.13
41.	MCULE-5302780192	No	No	No	No	1	0.55	0	0	2	3.28
42.	MCULE-40638207	No	No	No	No	No	0.55	0	0	No	3.12

	06										
43.	MCULE-1726158340	No	No	No	No	No	0.55	0	1	1	3.06
44.	MCULE-9917566553	No	No	No	No	No	0.55	0	0	1	1.88
45.	MCULE-7280319389	No	No	No	No	No	0.55	0	0	1	2.53
46.	Tucatinib - inhibitor	No	2	No	No	No	0.55	0	0	2	4.01
47.	Lapatinib - inhibitor	1	3	1	1	1	0.55	0	0	3	4.05
48.	Neratinib - inhibitor	1	2	1	No	No	0.55	0	1	3	4.08

[*]BS: Bioavailability score (Compounds satisfying RO5 with a BS of 0.55 considered as an excellent oral absorption);

[^]PS: PAINS; [&]BK: Brenk; [#]LL: Leadlikeness; [$]SA: Synthetic accessibility (1: very easy, 10: very difficult)

Molecular Docking

AutoDock Vina

All ligand hits (45) and reference inhibitors (Lapatinib, Neratinib and Tucatinib) were docked to HER2 using MCULE's ADV tool to assess their binding affinities in terms of binding free energy (ΔG). Among inhibitors, Tucatinib (ΔG: -8.22 kcal/mol) was found as the best molecule interacting efficiently with target protein HER2, followed by Neratinib (-8.12 kcal/mol) and Lapatinib (-7.7 kcal/mol). Eleven ligand hits viz., Mcule-9083675198 (-9.9 kcal/mol), Mcule-2082061687 (-9.8 kcal/mol), Mcule-9514587152 (-9.7 kcal/mol), Mcule-8016227151 (-9.5 kcal/mol), Mcule-4420319124 (-9.1 kcal/mol), Mcule-7002197612 (-9.0 kcal/mol), Mcule-3840783663 (-8.9 kcal/mol), Mcule-4544985274 (-8.9

kcal/mol), Mcule-9433162170 (-8.8 kcal/mol), Mcule-8028742001 (-8.8 kcal/mol), and Mcule-4638340739 (-8.8 kcal/mol) was showing better binding interactions as compared to the Tucatinib (Table 4.8).

Table 4.8: Molecular interaction analysis of top eleven ligand hits and reference inhibitors.

S. No.	**Ligand**	**AutoDock Vina ΔG (kcal/mol)**
1.	MCULE-9083675198	-9.9
2.	MCULE-2082061687	-9.8
3.	MCULE-9514587152	-9.7
4.	MCULE-8016227151	-9.5
5.	MCULE-4420319124	-9.1
6.	MCULE-7002197612	-9.0
7.	MCULE-3840783663	-8.9
8.	MCULE-4544985274	-8.9
9.	MCULE-9433162170	-8.8
10.	MCULE-8028742001	-8.8
11.	MCULE-4638340739	-8.8
12.	Tucatinib- inhibitor	-8.22
13.	Neratinib- inhibitor	-8.12
14.	Lapatinib- inhibitor	-7.76

AutoDock Vina method is used to identify potential drug candidates comparatively better than reference inhibitors. The 3 D shape of molecules and holding forces are crucial features in the molecular interaction of two molecules. During binding interactions, energy is released, and conventionally it is defined as a negative sign, which means the more significant the energy released, the stronger the binding. Based on ΔG values eleven ligand hits were identified as more potent as compared to reference inhibitor Tucatinib (Table 6). Top two ligands viz., Mcule-9083675198 (-9.9 kcal/mol), Mcule-2082061687 (-9.8 kcal/mol), and best reference inhibitor, i.e., Tucatinib (ΔG: -8.22 kcal/mol) were carried forward for MD simulation study of 10 ns duration.

Molecular dynamics simulation

To assess the stability of docked complexes of top two hits Mcule-9083675198 (-9.9 kcal/mol), Mcule-2082061687 (-9.8 kcal/mol) , and known inhibitor Tucatinib with HER2, MD simulation run of 10 ns duration were executed using GROMACS package. MD plots for RMSD, RMSF, SASA, ΔGsolv, and Rg, were generated to evaluate the molecular interaction stability of ligands and protein complexes (Ali S et al., 2019, Kuzmanic A et al., 2010) .The binding of ligands into the binding pocket of HER2 acquires conformational changes to attain stability.

Average potential energy of system

The average potential energy (PE) of HER2-Tucatinib, HER2-Mcule-9083675198, and HER2-Mcule-2082061687 was estimated to determine the stability of the systems. The constant temperature fluctuations at 300 K for each system recommended a steady and precise MD simulation performed. The computed average PE of the above systems (-573444 kJ/mol, -573064kJ/mol, and -572962 kJ/mol, respectively) was comparable during the entire duration of 10 ns MD process (Table 4.9).

Table 4.9: Calculated parameters for all the systems obtained after 10 ns MD simulation.

Complexes	**Average PE (kJ/mol)**	**Average RMSD (nm)**	**Average RMSF (nm)**	**Average SASA (nm^2)**	**ΔGsolv (kJ/mol/nm^2)**	**Rg (nm)**	**Volume (nm^3)**	**Density (kg/m^3)**
Tucatinib	-573444	0.258966	0.084687	12.66534	-16.5483	1.991941	436.141	1036.26
MCULE-208206168	-572962	0.226329	0.098466	12.62438	-16.6734	1.992155	436	1036.71
MCULE-908367	-573064	0.250794	0.091428	12.62481	-16.6172	2.014734	436.164	1036.57

5198								

Root-mean-square deviation

RMSD measures the protein's stability and resemblance to its native structure. The average RMSD for Tucatinib (black), Mcule-2082061687 (red), Mcule-9083675198 (green), complexed with HER2 was found 0.258 nm, 0.226 nm, and 0.250 nm, respectively (Table 7). The RMSD plot reveals that the stability of docked complex of HER2 and ligand hits is comparable to known inhibitor Tucatinib (Figure 4.2).

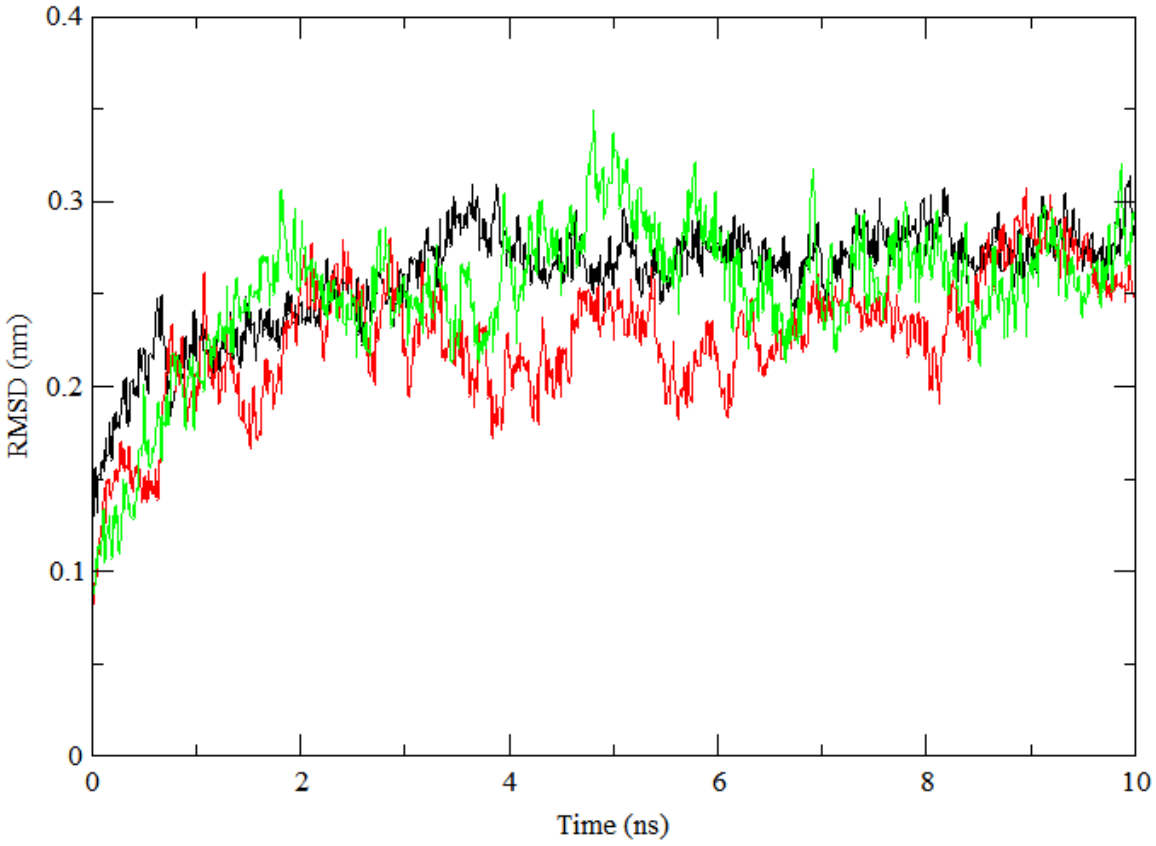

Figure 4.2. RMSD plot as a function of time. Black, red, and green colors represent values obtained for HER2-Tucatinib, HER2-Mcule-2082061687, and HER2-Mcule-9083675198, respectively.

Root-mean-square fluctuation

The RMSF graph ensures the stability of protein docked with ligand molecules during the entire period of MD simulation. Residues fluctuations at different sites in the RMSF plot are due to the molecular interaction of reference inhibitor and selected ligand hits. Average residues fluctuation upon binding with Mcule-2082061687 (0.226) (red), Mcule-9083675198 (0.50) (green), was found lesser than Tucatinib (0.258 nm) (black) (Figure 4.3).

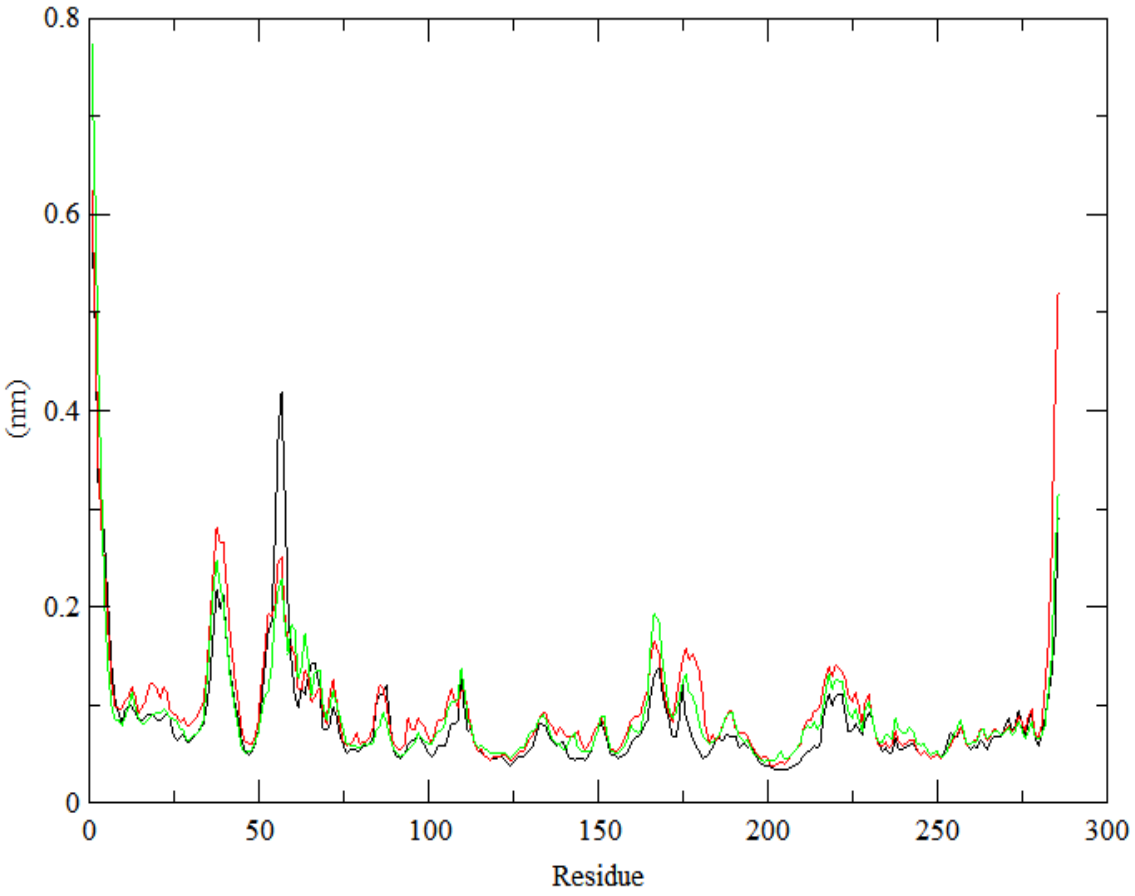

Figure 4.3. RMSF plot for HER2-Tucatinib (black), HER2-Mcule-2082061687 (Red), and KIFC1-Mcule-9083575198 (green).

Solvent-accessible surface area

The SASA plot exposes protein's interactable surface area to the solvent molecules. The average value of SASA for Tucatinib (black), Mcule- 208206168 (red), and Mcule-9083675198 (green), docked with HER2 was found as 12.66 nm^2, 12.62 nm^2, and 12.62 nm^2 (Figure 3.4, Table 7). The SASA findings exhibit that internal residues of HER2 upon

binding with Mcule-208206168 and Mcule-9083675198 is less accessible by the solvent than Tucatinib.

Free energy of solvation

The average ΔGsolv of HER2-Tucatinib (black), HER2-Mcule-208206168 (red), and HER2-Mcule- 9083675198 (green) was depicted as -16.548 kJ/mol/nm2, -16.673 kJ/mol/nm2, and -16.617 kJ/mol/nm2 respectively (Figure 4.4, Table 4.7).

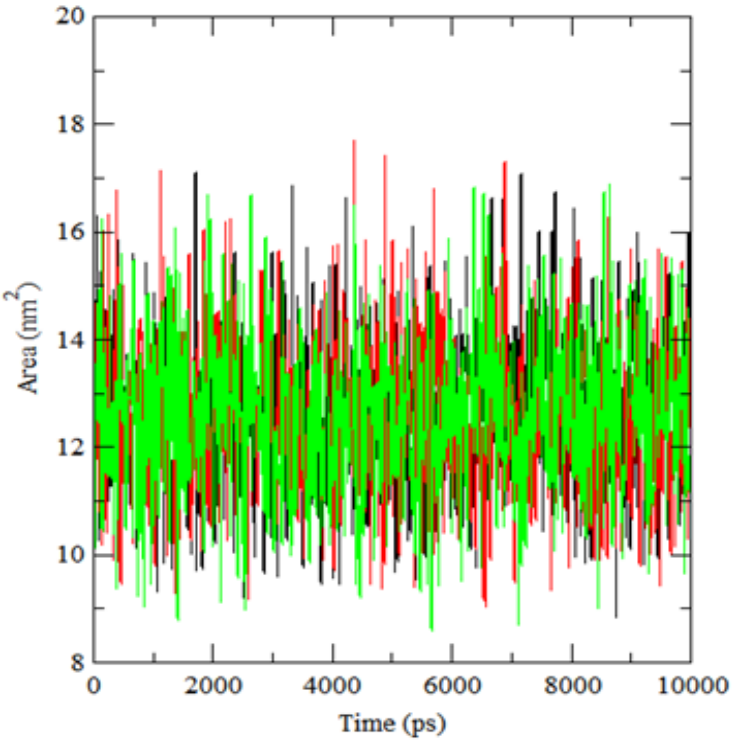

Figure 4.4. SASA plot for HER2-Tucatinib (black), HER2-Mcule-2082061687 (Red), and KIFC1-Mcule-9083575198 (green).

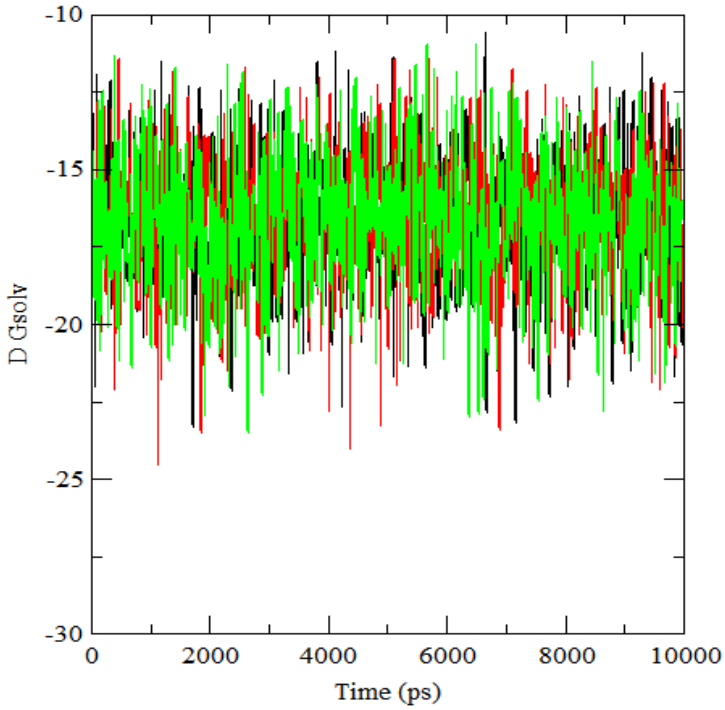

Figure 4.5. ΔGsolv plot for HER2-Tucatinib (black), HER2-Mcule-2082061687 (Red), and KIFC1-Mcule-9083575198 (green).

Radius of gyration

The Rg forecast the stability of target protein in a biological system and is associated to the compactness of the protein. The order of protein compactness is inversely related to Rg, means higher the compactness lesser is the Rg value. The average Rg of HER2-Tucatinib (black), HER2-Mcule-208206168 (red), and HER2-Mcule-9083675198 (green) was portrayed as -1.991 nm, 1.992 nm, and 2.014 nm respectively (Figure 4.6, Table 4.7). The average Rg values of inhibitor and ligand hits were almost equal during the entire process of MD simulation.

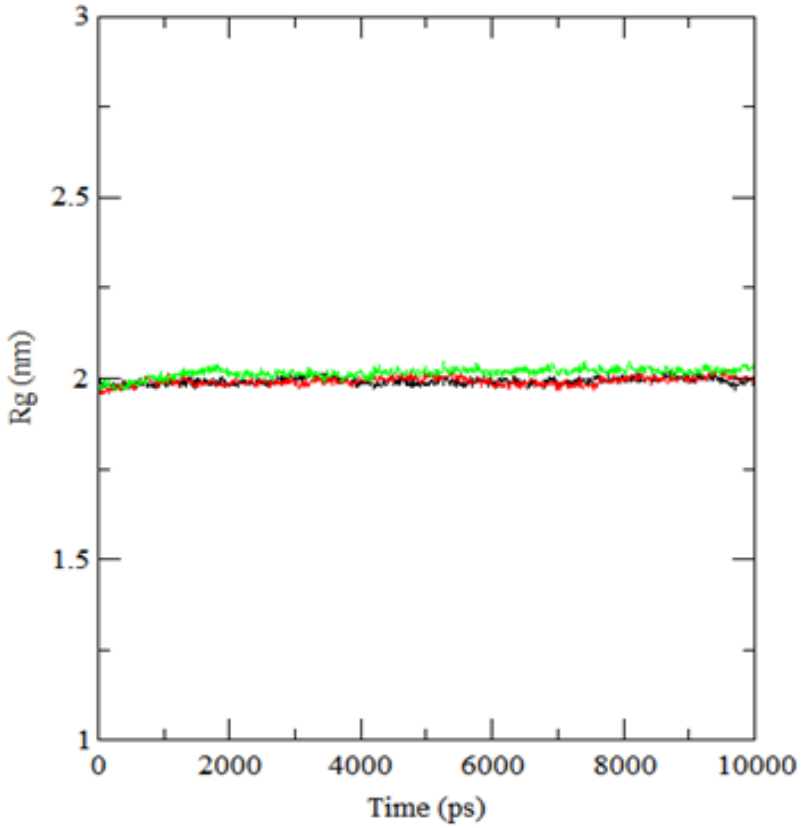

Figure 4.6. Rg plot for HER2-Tucatinib (black), HER2-Mcule-2082061687 (Red), and HER2-Mcule-9083575198 (green).

About 10 million people lost their lives worldwide due to cancer in 2020, as per the statistics of WHO. Breast, lung, colon and rectum, prostate, and skin cancers were the key drivers aggravating the situation in terms of new cases, especially in low- and middle-income countries. Despite the development of high-throughput technology and innovation in the data-powered healthcare system, it is also desirable to identify new prophylactically and therapeutically promising drug candidates against a target that affects the root cause of disease. HER2 is a multifaceted targetable tyrosine overexpressed in various cancer, and its knockdown facilitates the onset of apoptosis without damaging normal cells. So, in the study, 202,932,82 small molecules from MCULE's more than 5 million chemical repositories were identified using SBVS, which further reduced to 49 and 39 ligand hits after toxicity and BOILED-Egg filtration, respectively (Figure 4.1). Based on the CΔG values, a total of 10 ligands were identified, showing strong binding interaction with HER2 compared to Tucatinib, the most potent among reference inhibitors (Table 4.6). TRP181, ASP140, and

PHE26 residues of HER2 α4/α6 cleft were reported as a critical player responsible for ATP binding to the HER2-MT complex and dissociation of ATP/ADP from the complex. Post docking analysis reveals that Tucatinib, and Mcule-2082061687 are docked with TRP181, GLY28 and PHE26 residues of KIFC1 α4/α6 cleft, while Mcule-9083575198 showed interaction with other residues rather than TRP181, GLY28 and PHE26. Details of molecular binding types and active residues are shown in Figures 4.7- 4.9.

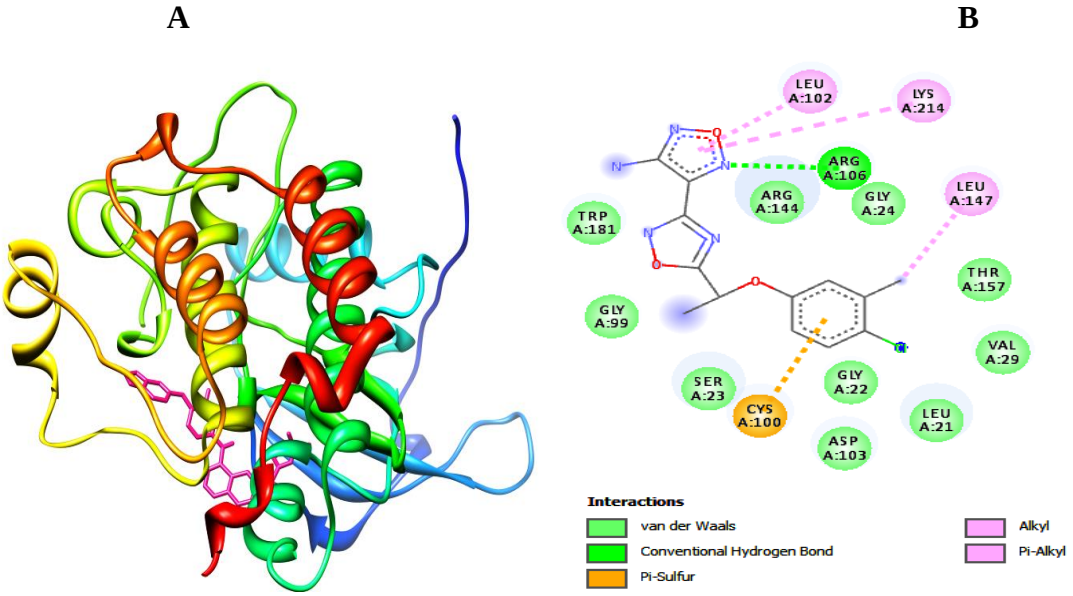

Figure 4.7. HER2-Tucatinib (reference inhibitor) complex. **A)** 3D view of the Tucatinib (red sticks) bound to the α4/α6 cleft of HER2. **B)** 2D diagram showing the HER2 residues that bind to Tucatinib. The internal legend indicates the bond type by color. Amino acid residues are shown in 3-letter code; the number indicates the position within the chain, and the capital letters (A) indicate which chain the residue belongs to.

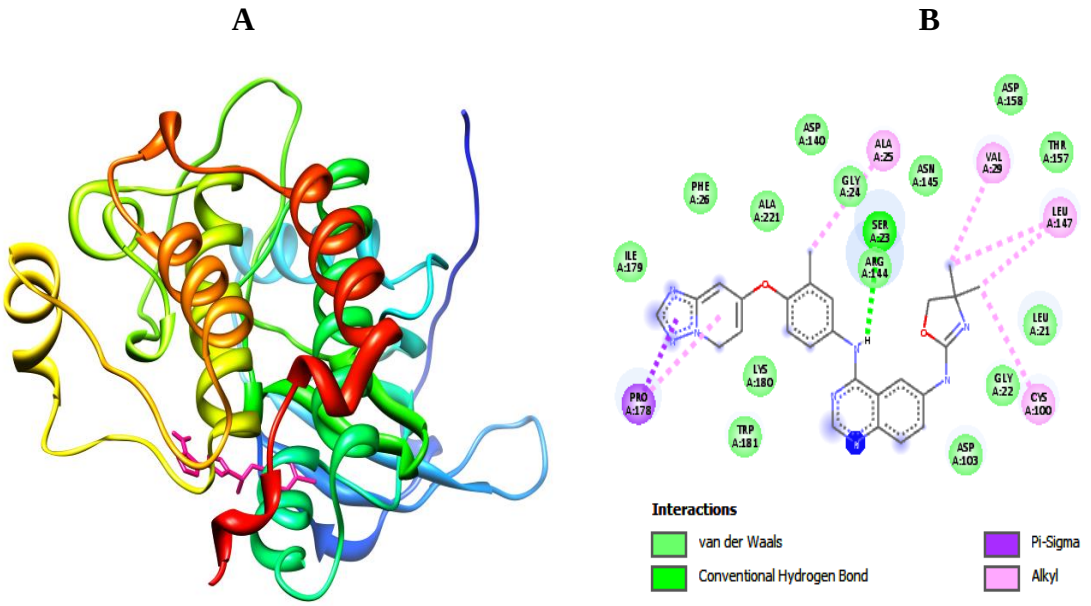

Figure 4.8. HER2- Mcule-2082061687 complex. **A)** 3D view of the Mcule-2082061687 (red sticks) bound to the α4/α6 cleft of HER2. **B)** 2D diagram showing the HER2 residues that bind to Mcule-2082061687. The internal legend indicates the bond type by color. Amino acid residues are shown in 3-letter code; the number indicates the position within the chain, and the capital letters (A) indicate which chain the residue belongs to.

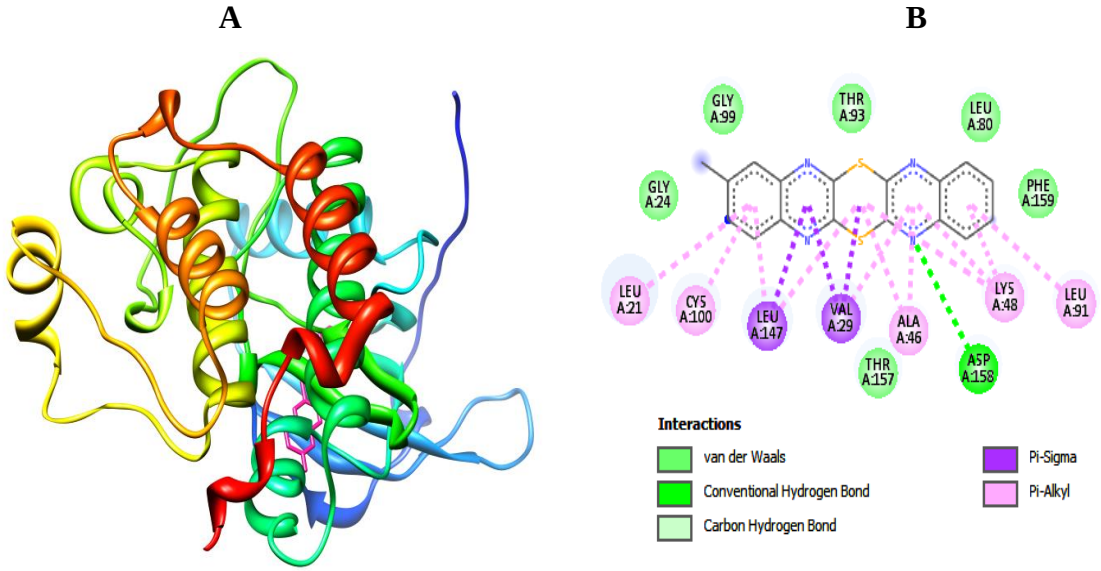

Figure 4.9. HER2- Mcule-9083575198 complex. **A)** 3D view of the Mcule-9083575198 (red sticks) bound to the α4/α6 cleft of KIFC1. **B)** 2D diagram showing the KIFC1 residues that bind to Mcule-4895338547. The internal legend indicates the bond type by color. Amino acid

residues are shown in 3-letter code; the number indicates the position within the chain, and the capital letters (A) indicate which chain the residue belongs to.

During MD simulation of 10 ns duration, RMSD analysis HER2 backbone, ligand hits, reference inhibitor, and their respective complexes forecast that Mcule-9083575198 upon binding with HER2 remains stable in comparison of Tucatinib, while remaining ligand, e.g., Mcule-2082061687 deviated upon binding.

Principal Component Analysis

PCA is employed to examine the relationship between different conformers/structures based on their equivalent residues. The application of PCA to both distributions of experimental structures and Molecular Dynamics trajectories, along with its ability to provide considerable insight into the nature of conformational differences in a range of protein families and other biomolecules (Munjal N. S et al., 2021).

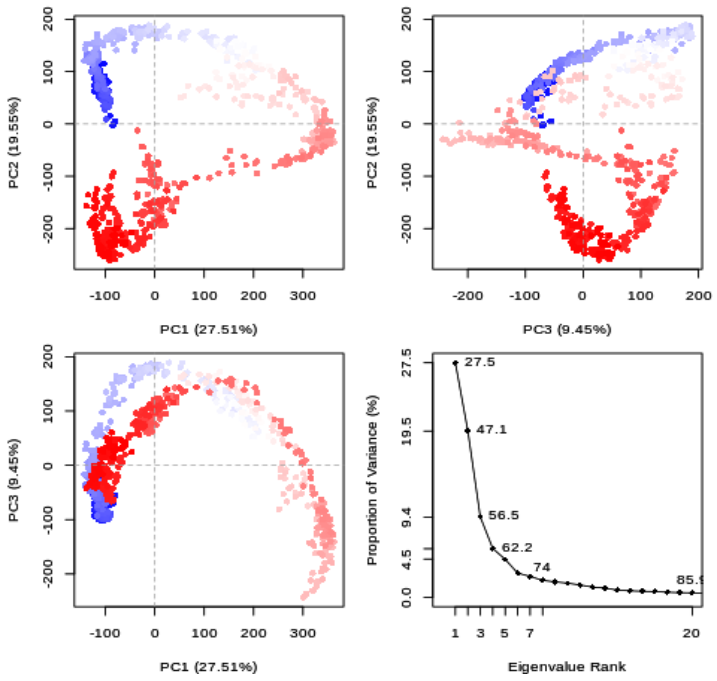

Figure 4.10. PCA: HER2-Tucatinib

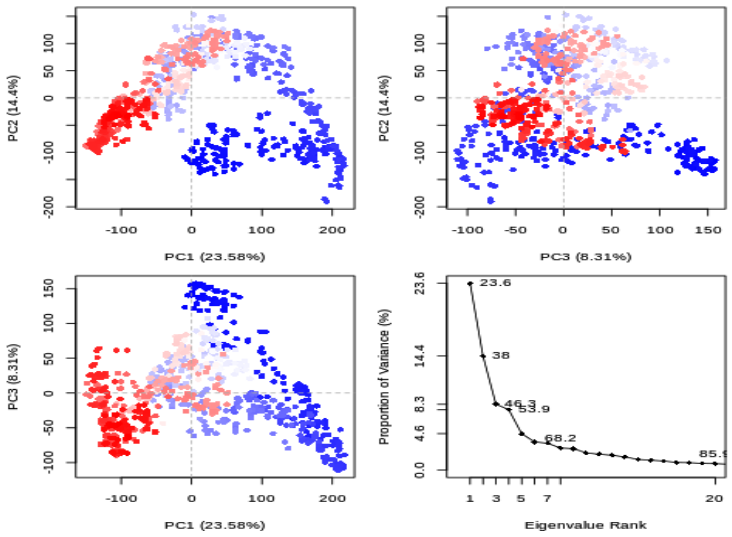

Figure 4.11. PCA: HER2-Mcule-9083575198

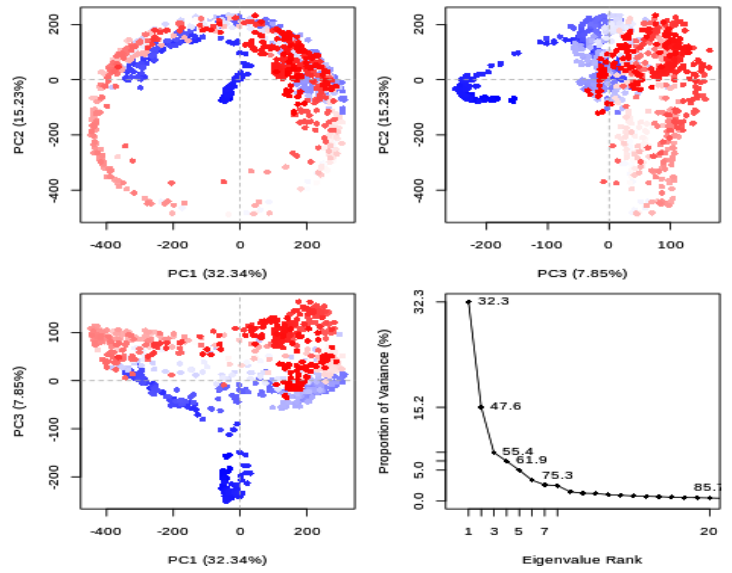

Figure 4.12. PCA: HER2-Mcule-2082061687

Molecular interaction of HER2 and reference inhibitor Tucatinib shows seven types of binding interactions viz., van der Waals, carbon-hydrogen bond, halogen (fluorine), pi-sigma, pi-sulfur, alkyl, and pi-alkyl. All five rings of Tucatinib were found engaged in molecular interaction with eleven residues of HER2 α4/α6 cleft (Figure 3.10). Compared to the HER2-Tucatinib complex, the HER2- Mcule-9083575198 complex was depicted as more stable

with six types of interactions, including van der Waals, carbon-hydrogen bond, halogen (fluorine), pi-pi T-shaped, alkyl, and pi-alkyl. Moreover, all five rings of the Mcule-9083575198 were found engaged in molecular interaction of fourteen residues of α4/α6 cleft (GLY99, THR93, LEU80, LEU21, CYS100, LEU1447, VAL29, ALA46, ASP159, LYS48, LEU91, GLY24 THR159, ASP157, and PHE159,) (Figure 4.9). It can be inferred from the study that the protein HER2 upon binding with Mcule-9083675198 would be unable to interact with various proteins involved in cell cycle progression and mitosis, e.g., PRC1, CDC20, CDK1, PLK1, TPX2, NUSAP1, and MAD2L1 that subsequently hinder bipolar division, avert cell proliferation, induce cell cycle arrest, and thus facilitating the apoptosis of cancer cells. An outline of the HER2 inhibition mechanism through known inhibitors and Mcule-9083575198 is illustrated in Figure 4.13.

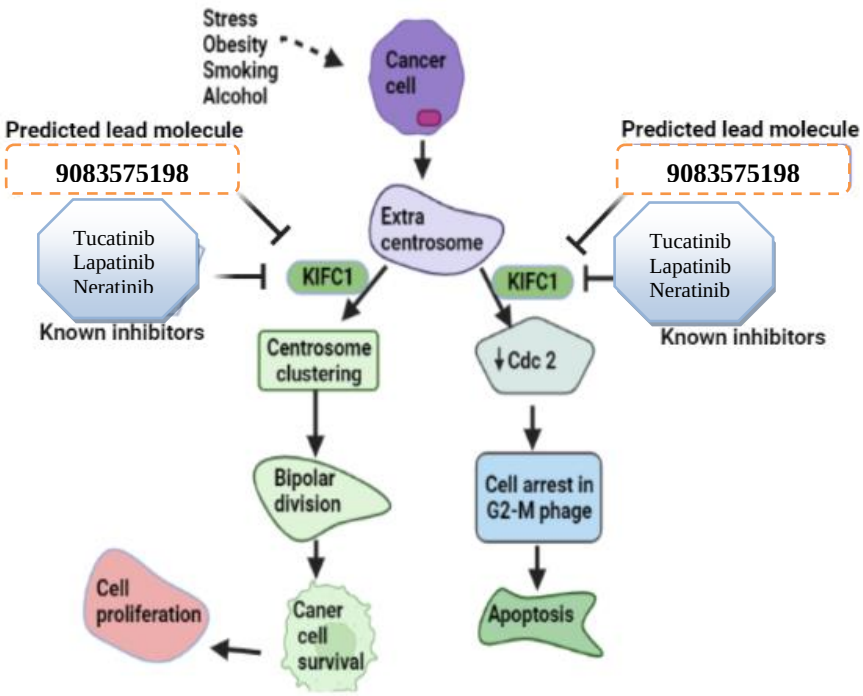

Figure 4.13. HER2 inhibition mechanism by known inhibitors (Tucatinib, Lapatinib, and Neratinib), and predicted lead molecule Mcule-9083575198.

5. CONCLUSIONS

The Mcule-9083675198 showed a significant binding propensity towards HER2 α4/α6 cleft, indicating stability and consequent effectiveness in inhibiting target protein better than reference inhibitor Tucatinib. The Mcule-2082061687 also exhibited plausible inhibition potential compared to Tucatinib, but their complexes were found unstable during the MD simulation process. Physicochemical properties (MW: 334.42 g/mol, RB: 4, MR: 92.29, TPSA: 102.16 Å2), lipophilicity (XLogP3: 4.85, WLogP: 4.5, MLogP: 2.8), solubility (Log S (ESOL): -5.61), Log S (Ali): -6.73), Log S (SILICOS-IT): -7.35), druglikeness (violation of RO5, Ghose, Veber, Egan, and Muegge: none), medicinal chemistry attributes (PS and BK alert: none, LL: 1, SA: 3.05) of Mcule-9083675198 are far better than Physicochemical properties (MW: 480.52 g/mol, RB: 6, MR: 141.66, TPSA: 110.85 Å2), lipophilicity (XLogP3: 3.99, WLogP: 4.52, MLogP: 3.01), solubility (Log S (ESOL): -5.45), Log S (Ali): -6.02), Log S (SILICOS-IT): -9.12), druglikeness (violation of RO5: none, Ghose: 2, Veber: none, Egan: none, and Muegge: none), medicinal chemistry attributes (PS and BK alert: none, LL: 2, SA: 4.01) of Tucatinib. The BS score (0.55) of both Mcule-2082061687 and Tucatinib is equal, which means that both have good oral absorption. In the purview of our research findings, it is elucidated that Mcule-9083675198 contains all therapeutic features as an excellent oral drug molecule and could be promising in cancer prevention and treatment via K-14F-based novel drug design and development.

6. REFERENCES

Aertsens, J., Mondelaers, K., Verbeke, W., Buysse, J., & Huylenbroeck, G. V. (2021). 2011. The influence of subjective and objective knowledge on attitude, motivations and consumption of organic food. British Food Journal 113 (11): 1353–1378. Afina, S. and Retnaningsih. 2018. The influence of students' knowledge and. Information and Management, 17(3), 31-46.

Ahmad, K. M. K., Salman, A., Al-Khodairy Salman, F., Al-Marshad Feras, M., Alshahrani Abdulrahman, M., & Arif Jamal, M. (2020). Computational Exploration of Dibenzo [a,l] Pyrene Interaction to DNA and its Bases: Possible Implications to Human Health. Biointerface Research in Applied Chemistry, 11(4), 11272–11283. https://doi.org/10.33263/BRIAC114.1127211283

Ajijur, R., Salman, A., & Ahmad, K. M. K. (2021). Combinatorial Design to Decipher Novel Lead Molecule against Mycobacterium tuberculosis. Biointerface Research in Applied Chemistry, 11(5), 12993–13004. https://doi.org/10.33263/BRIAC115.1299313004
Akram M, Siddiqui SA. Breast cancer management: past, present and evolving. Indian J Cancer. 2012;49(3):277–282.

Ali, J., Camilleri, P., Brown, M. B., Hutt, A. J., & Kirton, S. B. (2012). Revisiting the General Solubility Equation: In Silico Prediction of Aqueous Solubility Incorporating the Effect of Topographical Polar Surface Area. Journal of Chemical Information and Modeling, 52(2), 420–428. https://doi.org/10.1021/ci200387c

Ali, S., Khan, F., Mohammad, T., Lan, D., Hassan, M., & Wang, Y. (2019). Identification and Evaluation of Inhibitors of Lipase from Malassezia restricta using Virtual High-Throughput Screening and Molecular Dynamics Studies. International Journal of Molecular Sciences, 20(4), 884. https://doi.org/10.3390/ijms20040884

Anurag M, Zhu M, Huang C, Vasaikar S, Wang J, Hoog J, Burugu S, Gao D, Suman V, Zhang XH, Zhang B. Immune checkpoint profiles in luminal B breast cancer (Alliance). JNCI: Journal of the National Cancer Institute. 2020 Jul;112(7):737-46.

Anurag M, Zhu M, Huang C, Vasaikar S, Wang J, Hoog J, Burugu S, Gao D, Suman V, Zhang XH, Zhang B. Immune checkpoint profiles in luminal B breast cancer (Alliance). JNCI: Journal of the National Cancer Institute. 2020 Jul;112(7):737-46.

Arteaga CL, Sliwkowski MX, Osborne CK, Perez EA, Puglisi F, Gianni L. Treatment of HER2-positive breast cancer: current status and future perspectives. Nature reviews Clinical oncology. 2012 Jan;9(1):16-32.

Attique, S., Hassan, M., Usman, M., Atif, R., Mahboob, S., Al-Ghanim, K., … Nawaz, M. (2019). A Molecular Docking Approach to Evaluate the Pharmacological Properties of Natural and Synthetic Treatment Candidates for Use against Hypertension. International Journal of Environmental Research and Public Health, 16(6), 923. https://doi.org/10.3390/ijerph16060923

Aziz SW, Aziz MH. Major signaling pathways involved in breast cancer. InBreast cancer metastasis and drug resistance 2013 (pp. 47-64). Springer, New York, NY.

Baell, J. B., & Holloway, G. A. (2010). New Substructure Filters for Removal of Pan Assay Interference Compounds (PAINS) from Screening Libraries and for Their Exclusion in Bioassays. Journal of Medicinal Chemistry, 53(7), 2719–2740. https://doi.org/10.1021/jm901137j

Bas, D. C., Rogers, D. M., & Jensen, J. H. (2008). Very fast prediction and rationalization of pKa values for protein-ligand complexes. Proteins: Structure, Function, and Bioinformatics, 73(3), 765–783. https://doi.org/10.1002/prot.22102

Bhat V, Roshini AP, Ramesh R. Does quality of life among modified radical mastectomy and breast conservation surgery patients differ? A 5-year comparative study. Indian Journal of Surgical Oncology. 2019 Dec;10(4):643-8.

Bremer, A., Wik, E., & Akslen, L. A. (2022). HER2 Revisited: Reflections on the Future of Cancer Biomarker Research. In Precision Oncology and Cancer Biomarkers (pp. 97-119). Springer, Cham.

Brenk, R., Schipani, A., James, D., Krasowski, A., Gilbert, I. H., Frearson, J., & Wyatt, P. G. (2008). Lessons Learnt from Assembling Screening Libraries for Drug Discovery for Neglected Diseases. ChemMedChem, 3(3), 435–444. https://doi.org/10.1002/cmdc.200700139

Chatterjee N, Walker GC. Mechanisms of DNA damage, repair, and mutagenesis. Environmental and molecular mutagenesis. 2017 Jun;58(5):235-63.

Chen, J., & Sun, L. (2012). Formononetin-induced apoptosis by activation of Ras/p38 mitogen-activated protein kinase in estrogen receptor-positive human breast cancer cells. Hormone and Metabolic Research, 44(13), 943-948.

Daina, A., Michielin, O., & Zoete, V. (2017). SwissADME: a free web tool to evaluate pharmacokinetics, drug-likeness and medicinal chemistry friendliness of small molecules. Scientific Reports, 7(1), 42717. https://doi.org/10.1038/srep42717

Davis, M. I., Hunt, J. P., Herrgard, S., Ciceri, P., Wodicka, L. M., Pallares, G., ... & Zarrinkar, P. P. (2011). Comprehensive analysis of kinase inhibitor selectivity. Nature biotechnology, 29(11), 1046-1051.

Demonty, G., Bernard-Marty, C., Puglisi, F., Mancini, I., & Piccart, M. (2007). Progress and new standards of care in the management of HER-2 positive breast cancer. European Journal of Cancer, 43(3), 497-509.

Dong Y, Li W, Gu Z, Xing R, Ma Y, Zhang Q, Liu Z. Inhibition of HER2-positive breast cancer growth by blocking the HER2 signaling pathway with HER2-glycan-imprinted nanoparticles. Angewandte Chemie International Edition. 2019 Jul 29;58(31):10621-5.

Dong, Y., Li, W., Gu, Z., Xing, R., Ma, Y., Zhang, Q., & Liu, Z. (2019). Inhibition of HER2-positive breast cancer growth by blocking the HER2 signaling pathway with HER2-glycan-imprinted nanoparticles. Angewandte Chemie International Edition, 58(31), 10621-10625.

Effiong, E. B., Nweke, B. C., Okereke, A. H., & Pius, A. N. O. (2022). BREAST CANCER–REVIEW. Journal of Global Biosciences Vol, 11(3), 9248-9257.

Effiong, E. B., Nweke, B. C., Okereke, A. H., & Pius, A. N. O. (2022). BREAST CANCER–REVIEW. Journal of Global Biosciences Vol, 11(3), 9248-9257.

Egan, W. J., & Lauri, G. (2002). Prediction of intestinal permeability. Advanced Drug Delivery Reviews, 54(3), 273–289. https://doi.org/10.1016/S0169-409X(02)00004-2

Egan, W. J., Merz, K. M., & Baldwin, J. J. (2000). Prediction of Drug Absorption Using Multivariate Statistics. Journal of Medicinal Chemistry, 43(21), 3867–3877. https://doi.org/10.1021/jm000292e

Eltayeb, T. F. (2014). Detection of breast cancer using artificial neural networks (ANN) (Doctoral dissertation, Sudan University of Science and Technology).

Ertl, P., & Schuffenhauer, A. (2009). Estimation of synthetic accessibility score of drug-like molecules based on molecular complexity and fragment contributions. Journal of Cheminformatics, 1(1), 8. https://doi.org/10.1186/1758-2946-1-8

Ertl, P., Rohde, B., & Selzer, P. (2000). Fast Calculation of Molecular Polar Surface Area as a Sum of Fragment-Based Contributions and Its Application to the Prediction of Drug Transport Properties. Journal of Medicinal Chemistry, 43(20), 3714–3717. https://doi.org/10.1021/jm000942e

Fan, X. W., Zang, Y., Xi, L., & Li, S. D. (2015). The Emodin inducted human breast cancer MCF-7cell apoptosis and activated JNK signal transduction pathways. J. Chin. J. Surg. Oncol, 7(06), 346-350.

Fischer, N. M., van Maaren, P. J., Ditz, J. C., Yildirim, A., & van der Spoel, D. (2015). Properties of Organic Liquids when Simulated with Long-Range Lennard-Jones Interactions. Journal of Chemical Theory and Computation, 11(7), 2938–2944. https://doi.org/10.1021/acs.jctc.5b00190

Fukada I, Araki K, Kobayashi K, Shibayama T, Takahashi S, Gomi N, Kokubu Y, Oikado K, Horii R, Akiyama F, Iwase T. Pattern of tumor shrinkage during neoadjuvant chemotherapy is associated with prognosis in low-grade luminal early breast cancer. Radiology. 2018 Jan;286(1):49-57.

Fukada I, Araki K, Kobayashi K, Shibayama T, Takahashi S, Gomi N, Kokubu Y, Oikado K, Horii R, Akiyama F, Iwase T. Pattern of tumor shrinkage during neo adjuvant chemotherapy is associated with prognosis in low-grade luminal early breast cancer. Radiology. 2018 Jan;286(1):49-57.

Ghauri, M. A., Raza, A., Hayat, U., Atif, N., Iqbal, H. M., & Bilal, M. (2022). Mechanistic insights expatiating the biological role and regulatory implications of estrogen and HER2 in breast cancer metastasis. Biochimica et Biophysica Acta (BBA)-General Subjects, 130113.

Ghose, A. K., Viswanadhan, V. N., & Wendoloski, J. J. (1999). A Knowledge-Based Approach in Designing Combinatorial or Medicinal Chemistry Libraries for Drug Discovery.

1. A Qualitative and Quantitative Characterization of Known Drug Databases. Journal of Combinatorial Chemistry, 1(1), 55–68. https://doi.org/10.1021/cc9800071

Gonçalves Jr H, Guerra MR, Duarte Cintra JR, Fayer VA, Brum IV, Bustamante Teixeira MT. Survival study of triple-negative and non–triple-negative breast cancer in a Brazilian Cohort. Clinical Medicine Insights: Oncology. 2018 Jul 26;12:1179554918790563.

Gupta, S., Chahar, B. S., & Puja, K. (2021). Changing pattern of female cancer during last 10 years-experience from a Tertiary Cancer Center. International Journal of Science and Research Archive, 2(2), 018-027..

Hashmi AA, Aijaz S, Khan SM, Mahboob R, Irfan M, Zafar NI, Nisar M, Siddiqui M, Edhi MM, Faridi N, Khan A. Prognostic parameters of luminal A and luminal B intrinsic breast cancer subtypes of Pakistani patients. World journal of surgical oncology. 2018 Dec;16(1):1-6.

Hashmi AA, Aijaz S, Khan SM, Mahboob R, Irfan M, Zafar NI, Nisar M, Siddiqui M, Edhi MM, Faridi N, Khan A. Prognostic parameters of luminal A and luminal B intrinsic breast cancer subtypes of Pakistani patients. World journal of surgical oncology. 2018 Dec;16(1):1-6.

Hermansyah, D., & Firsty, N. N. (2022). The Role of Breast Imaging in Pre-and Post-Definitive Treatment of Breast Cancer. Exon Publications.

Hevener, K. E. (2018). Computational Toxicology Methods in Chemical Library Design and High-Throughput Screening Hit Validation. In Methods in Molecular Biology (Vol. 1800, pp. 275–285). https://doi.org/10.1007/978-1-4939-7899-1_13

https://www.mayoclinic.org/diseases-conditions/breast-cancer/in-depth/breast-cancer/art-20045654

https://www.mayoclinic.org/diseases-conditions/breast-cancer/in-depth/breast-cancer/art-20045654

https://www.who.int/news-room/fact-sheets/detail/breast

Khan, F. I., Lai, D., Anwer, R., Azim, I., & Khan, M. K. A. (2020). Identifying novel sphingosine kinase 1 inhibitors as therapeutics against breast cancer. Journal of Enzyme Inhibition and Medicinal Chemistry, 35(1), 172–186. https://doi.org/10.1080/14756366.2019.1692828

Khan, M. K. A., Akhtar, S., & Arif, J. M. (2018). Development of In Silico Protocols to Predict Structural Insights into the Metabolic Activation Pathways of Xenobiotics. Interdisciplinary Sciences: Computational Life Sciences, 10(2), 329–345. https://doi.org/10.1007/s12539-017-0237-4

Khan, M. K. A., Akhtar, S., & Arif, J. M. (2018). Structural Insight into the Mechanism of Dibenzo[a,l]pyrene and Benzo[a]pyrene-Mediated Cell Proliferation Using Molecular Docking Simulations. Interdisciplinary Sciences: Computational Life Sciences, 10(4), 653–673. https://doi.org/10.1007/s12539-017-0226-7

Khan, M. K. A., Pokharkar, N. B., Al-Khodairy, F. M., Al-Marshad, F. M., & Arif, J. M. (2020). Structural Perspective on Molecular Interaction of IgG and IgA with Spike and Envelope Proteins of SARS-CoV-2 and Its Implications to Non-Specific Immunity. Biointerface Research in Applied Chemistry, 11(3), 10923–10939. https://doi.org/10.33263/BRIAC113.1092310939

Khuwaja GA, Abu-Rezq AN. Bimodal breast cancer classification system. Pattern analysis and applications. 2004 Sep;7(3):235-42.

Kiss, R., Sandor, M., & Szalai, F. A. (2012). http://Mcule.com: a public web service for drug discovery. Journal of Cheminformatics, 4(S1), P17. https://doi.org/10.1186/1758-2946-4-S1-P17

Kovacs, T., Zakany, F., & Nagy, P. (2022). It Takes More than Two to Tango: Complex, Hierarchal, and Membrane-Modulated Interactions in the Regulation of Receptor Tyrosine Kinases. Cancers, 14(4), 944.

Kuzmanic, A., & Zagrovic, B. (2010). Determination of Ensemble-Average Pairwise Root Mean-Square Deviation from Experimental B-Factors. Biophysical Journal, 98(5), 861–871. https://doi.org/10.1016/j.bpj.2009.11.011

Labani S, Asthana S, Srivastava A, Vohra P, Bhatia D. Incidence and trends of breast and cervical cancers: A Joinpoint regression analysis. Indian Journal of Medical and Paediatric Oncology. 2020 Jul;41(05):654-62.

Lipinski, C. A., Lombardo, F., Dominy, B. W., & Feeney, P. J. (2001). Experimental and computational approaches to estimate solubility and permeability in drug discovery and development settings. Advanced Drug Delivery Reviews, 46(1–3), 3–26. https://doi.org/10.1016/S0169-409X(00)00129-0

Liu, C., Zhang, K., Shen, H., Yao, X., Sun, Q., & Chen, G. (2018). Necroptosis: a novel manner of cell death, associated with stroke. International Journal of Molecular Medicine, 41(2), 624-630.

Loibl S, Gianni L. HER2-positive breast cancer. The Lancet. 2017 Jun 17;389(10087):2415-29.

Martin, Y. C. (2005). A Bioavailability Score. Journal of Medicinal Chemistry, 48(9), 3164–3170. https://doi.org/10.1021/jm0492002

Miricescu, D., Totan, A., Stanescu-Spinu, I. I., Badoiu, S. C., Stefani, C., & Greabu, M. (2020). PI3K/AKT/mTOR signaling pathway in breast cancer: From molecular landscape to clinical aspects. International journal of molecular sciences, 22(1), 173.

Mohammad, R. M., Muqbil, I., Lowe, L., Yedjou, C., Hsu, H. Y., Lin, L. T., ... & Azmi, A. S. (2015, December). Broad targeting of resistance to apoptosis in cancer. In Seminars in cancer biology (Vol. 35, pp. S78-S103). Academic Press.

Moriguchi, I., Hirono, S., Liu, Q., Nakagome, I., & Matsushita, Y. (1992). Simple Method of Calculating Octanol/Water Partition Coefficient. Chemical and Pharmaceutical Bulletin, 40(1), 127–130. https://doi.org/10.1248/cpb.40.127

Morris, G. M., Goodsell, D. S., Halliday, R. S., Huey, R., Hart, W. E., Belew, R. K., & Olson, A. J. (1998). Automated docking using a Lamarckian genetic algorithm and an empirical binding free energy function. Journal of Computational Chemistry, 19(14), 1639–1662. https://doi.org/10.1002/(SICI)1096-987X(19981115)19:14<1639::AID-JCC10>3.0.CO;2-B

Morris, G. M., Goodsell, D. S., Huey, R., & Olson, A. J. (1996). Distributed automated docking of flexible ligands to proteins: Parallel applications of AutoDock 2.4. Journal of Computer-Aided Molecular Design, 10(4), 293–304. https://doi.org/10.1007/BF00124499

Moulder, S. L., Yakes, F. M., Muthuswamy, S. K., Bianco, R., Simpson, J. F., & Arteaga, C. L. (2001). Epidermal growth factor receptor (HER1) tyrosine kinase inhibitor ZD1839 (Iressa) inhibits HER2/neu (erb B2)-overexpressing breast cancer cells in vitro and in vivo. Cancer research, 61(24), 8887-8895.

Muegge, I., Heald, S. L., & Brittelli, D. (2001). Simple Selection Criteria for Drug-like Chemical Matter. Journal of Medicinal Chemistry, 44(12), 1841–1846. https://doi.org/10.1021/jm015507e

Munjal, N. S., Shukla, R., & Singh, T. R. (2021). Physicochemical characterization of paclitaxel prodrugs with cytochrome 3A4 to correlate solubility and bioavailability implementing molecular docking and simulation studies. Journal of Biomolecular Structure and Dynamics, 1-13.

Murthy, R. K., Loi, S., Okines, A., Paplomata, E., Hamilton, E., Hurvitz, S. A., ... & Winer, E. P. (2020). Tucatinib, trastuzumab, and capecitabine for HER2-positive metastatic breast cancer. New England Journal of Medicine, 382(7), 597-609.

Nounou MI, ElAmrawy F, Ahmed N, Abdelraouf K, Goda S, Syed-Sha-Qhattal H. Breast cancer: conventional diagnosis and treatment modalities and recent patents and technologies. Breast cancer: basic and clinical research. 2015 Jan;9:BCBCR-S29420.

Nounou, M. I., ElAmrawy, F., Ahmed, N., Abdelraouf, K., Goda, S., & Syed-Sha-Qhattal, H. (2015). Breast cancer: conventional diagnosis and treatment modalities and recent patents and technologies. Breast cancer: basic and clinical research, 9, BCBCR-S29420.

O'Boyle, N. M., Banck, M., James, C. A., Morley, C., Vandermeersch, T., & Hutchison, G. R. (2011). Open Babel: An open chemical toolbox. Journal of Cheminformatics, 3(1), 33. https://doi.org/10.1186/1758-2946-3-33

OLEG TROTT, A. J. O., & Schroer, A. (2010). AutoDock Vina: Improving the Speed and Accuracy of Docking with a New Scoring Function, Efficient Optimization, and Multithreading. Journal of Computational Chemistry,31(2),455-61. https://doi.org/10.1002/jcc.21334

Pernas, S., Barroso-Sousa, R., & Tolaney, S. M. (2018). Optimal treatment of early stage HER2-positive breast cancer. Cancer, 124(23), 4455-4466.

Petersen, H. G. (1995). Accuracy and efficiency of the particle mesh Ewald method. The Journal of Chemical Physics, 103(9), 3668–3679. https://doi.org/10.1063/1.470043

Potts, R. O., & Guy, R. H. (1992). Predicting Skin Permeability. Pharmaceutical Research: An Official Journal of the American Association of Pharmaceutical Scientists, 9(5), 663–669. https://doi.org/10.1023/A:1015810312465

Rajabi, S., Maresca, M., Yumashev, A. V., Choopani, R., & Hajimehdipoor, H. (2021). The most competent plant-derived natural products for targeting apoptosis in cancer therapy. Biomolecules, 11(4), 534.

Rehm, J., Patra, J., & Popova, S. (2007). Alcohol drinking cessation and its effect on esophageal and head and neck cancers: a pooled analysis. International Journal of Cancer, 121(5), 1132-1137.

Roos WPKaina, B. (2012). DNA damage-induced apoptosis: From specific DNA lesions to the DNA damage response and apoptosis. Cancer Letters, 8.

Ruoxi, Z., Kang, R., & Daolin, T. (2021). The STING1 network regulates autophagy and cell death. Signal Transduction and Targeted Therapy, 6(1).

Russo, J., & Russo, I. H. (1980). Susceptibility of the mammary gland to carcinogenesis. II. Pregnancy interruption as a risk factor in tumor incidence. The American journal of pathology, 100(2), 497.

Russo, J., & Russo, I. H. (1980). Susceptibility of the mammary gland to carcinogenesis. II. Pregnancy interruption as a risk factor in tumor incidence. The American journal of pathology, 100(2), 497.

Ryzhov, A., Bray, F., Ferlay, J., Fedorenko, Z., Goulak, L., Gorokh, Y., ... & Znaor, A. (2020). Recent cancer incidence trends in Ukraine and short-term predictions to 2022. Cancer epidemiology, 65, 101663.

Seo, H. S., Ku, J. M., Choi, H. S., Woo, J. K., Jang, B. H., Shin, Y. C., & Ko, S. G. (2014). Induction of caspase-dependent apoptosis by apigenin by inhibiting STAT3 signaling in HER2-overexpressing MDA-MB-453 breast cancer cells. Anticancer research, 34(6), 2869-2882.

Shah, T., Shah, N., Vijay, D. G., Patel, B., & Patel, S. (2020). Male Breast Cancer: Current Trends—a Tertiary Care Centre Experience. Indian Journal of Surgical Oncology, 11(1), 7-11.

Shakil, S. (2019). Molecular interaction of investigational ligands with human brain acetylcholinesterase. Journal of Cellular Biochemistry, 120(7), 11820–11830. https://doi.org/10.1002/jcb.28461

Sharma GN, Dave R, Sanadya J, Sharma P, Sharma KK. Various types and management of breast cancer: an overview. Journal of advanced pharmaceutical technology & research. 2010 Apr;1(2):109.

Stenberg, S., & Stenqvist, B. (2020). An Exact Ewald Summation Method in Theory and Practice. The Journal of Physical Chemistry A, 124(19), 3943–3946. https://doi.org/10.1021/acs.jpca.0c01684

Street W. Breast cancer facts & figures 2019–2020. Am. Cancer Soc. 2019:1-38.

Tarar, M. Y., Inayat, S., Atta, R., Khurshid, S., Khan, A. A., & Hashmi, S. A. (2018). Knowledge and practices about breast cancer. Pakistan journal of surgery, 34(1), 17-24.

Teague, S. J., Davis, A. M., Leeson, P. D., & Oprea, T. (1999). The Design of Leadlike Combinatorial Libraries. Angewandte Chemie International Edition, 38(24), 3743–3748. https://doi.org/10.1002/(SICI)1521-3773(19991216)38:24<3743::AID-ANIE3743>3.0.CO;2-U

Turke AB, Song Y, Costa C, Cook R, Arteaga CL, Asara JM, Engelman JA. MEK inhibition leads to PI3K/AKT activation by relieving a negative feedback on ERBB receptors. Cancer research. 2012 Jul 1;72(13):3228-37.

Umar, A. M., Salman, A., Haris, S. M., & Kalim, K. M. (2021). Identification of potential lead molecules against dibenzo [a, l] pyrene-induced mammary cancer through targeting cytochrome P450 1A1, 1A2, and 1B1 isozymes. Biointerface Res Appl Chem, 12(1), 1096-109.https://doi.org/10.33263/BRIAC121.10961109

Van Der Spoel, D., Lindahl, E., Hess, B., Groenhof, G., Mark, A. E., & Berendsen, H. J. C. (2005). GROMACS: Fast, flexible, and free. Journal of Computational Chemistry, 26(16), 1701–1718. https://doi.org/10.1002/jcc.20291

Vanommeslaeghe, K., & MacKerell, A. D. (2012). Automation of the CHARMM General Force Field (CGenFF) I: Bond Perception and Atom Typing. Journal of Chemical Information and Modeling, 52(12), 3144–3154. https://doi.org/10.1021/ci300363c

Vanommeslaeghe, K., Hatcher, E., Acharya, C., Kundu, S., Zhong, S., Shim, J., … Mackerell, A. D. (2010). CHARMM general force field: A force field for drug-like molecules compatible with the CHARMM all-atom additive biological force fields. Journal of Computational Chemistry, 31(4), 671–690. https://doi.org/10.1002/jcc.21367

Veber, D. F., Johnson, S. R., Cheng, H.-Y., Smith, B. R., Ward, K. W., & Kopple, K. D. (2002). Molecular Properties That Influence the Oral Bioavailability of Drug Candidates. Journal of Medicinal Chemistry, 45(12), 2615–2623. https://doi.org/10.1021/jm020017n

Vincze O, Colchero F, Lemaître JF, Conde DA, Pavard S, Bieuville M, Urrutia AO, Ujvari B, Boddy AM, Maley CC, Thomas F. Cancer risk across mammals. Nature. 2022 Jan;601(7892):263-7.

Vuong D, Simpson PT, Green B, Cummings MC, Lakhani SR. Molecular classification of breast cancer. Virchows Archiv. 2014 Jul;465(1):1-4.

Vuong D, Simpson PT, Green B, Cummings MC, Lakhani SR. Molecular classification of breast cancer. VirchowsArchiv. 2014 Jul;465(1):1-4.

Wang J, Xu B. Targeted therapeutic options and future perspectives for HER2-positive breast cancer. Signal transduction and targeted therapy. 2019 Sep 13;4(1):1-22.

Watts, C. A., Richards, F. M., Bender, A., Bond, P. J., Korb, O., Kern, O., … Ley, S. V. (2013). Design, Synthesis, and Biological Evaluation of an Allosteric Inhibitor of HSET that Targets Cancer Cells with Supernumerary Centrosomes. Chemistry & Biology, 20(11), 1399–1410. https://doi.org/10.1016/j.chembiol.2013.09.012

Weigelt B, Geyer FC, Reis-Filho JS. Histological types of breast cancer: how special are they?. Molecular oncology. 2010 Jun 1;4(3):192-208.

Wu, J., Mikule, K., Wang, W., Su, N., Petteruti, P., Gharahdaghi, F., … Chen, H. (2013). Discovery and Mechanistic Study of a Small Molecule Inhibitor for Motor Protein KIFC1. ACS Chemical Biology, 8(10), 2201–2208. https://doi.org/10.1021/cb400186w

Yang, L., Li, Y., Bhattacharya, A., & Zhang, Y. (2019). A recombinant human protein targeting HER2 overcomes drug resistance in HER2-positive breast cancer. Science translational medicine, 11(476), eaav1620.

Ye, Z., Gao, D. L., Qin, Q., Ray, R. M., & Thomas, D. B. (2002). Breast cancer in relation to induced abortions in a cohort of Chinese women. British journal of cancer, 87(9), 977-981.
Yu, L., Strandberg, L., & Lenardo, M. J. (2008). The selectivity of autophagy and its role in cell death and survival. Autophagy, 4(5), 567-573.

Zhang, W., Zhai, L., Wang, Y., Boohaker, R. J., Lu, W., Gupta, V. V., … Li, Y. (2016). Discovery of a novel inhibitor of kinesin-like protein KIFC1. Biochemical Journal, 473(8), 1027–1035. https://doi.org/10.1042/BJ20150992

Zhang, Y. (2021). The root cause of drug resistance in HER2-positive breast cancer and the therapeutic approaches to overcoming the resistance. Pharmacology & Therapeutics, 218, 107677.

Zoete, V., Grosdidier, A., Cuendet, M., & Michielin, O. (2010). Use of the FACTS solvation model for protein-ligand docking calculations. Application to EADock. Journal of Molecular Recognition, 23(5), 457–461. https://doi.org/10.1002/jmr.1012